MAX-PLANCK-INSTITUT
FÜR PLASMAPHYSIK

X-point radiation and its up/down asymmetry in the detached plasma regime in Wendelstein 7-X

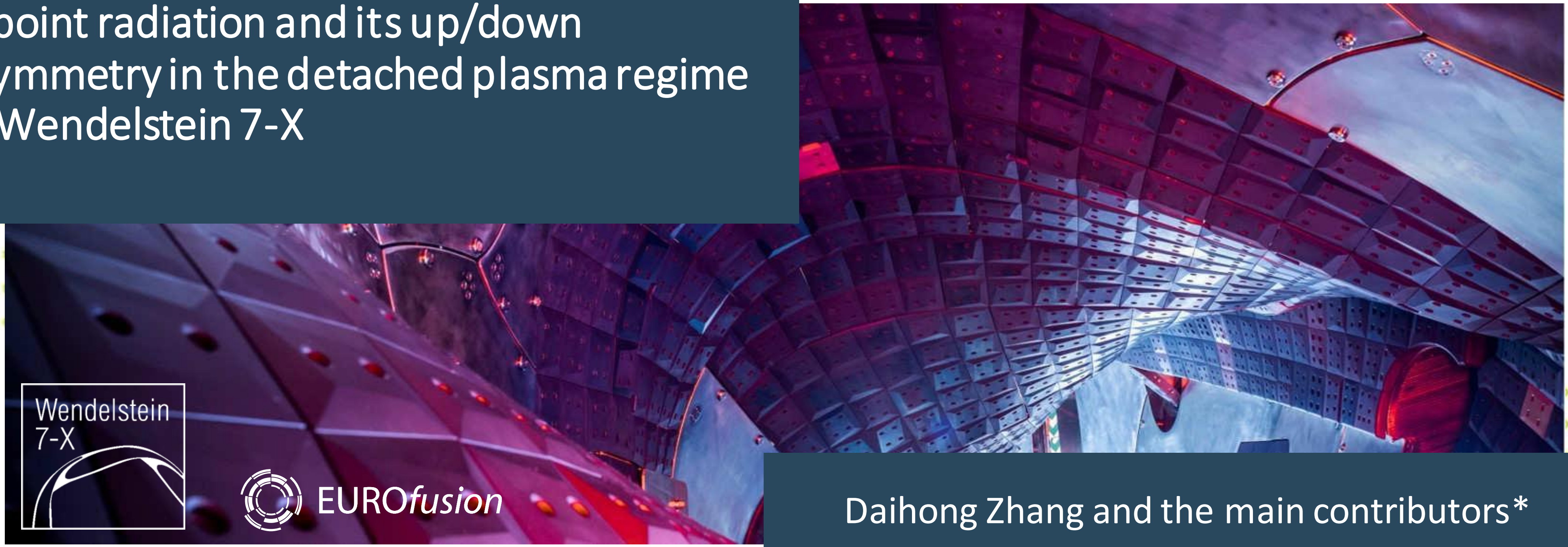

Daihong Zhang and the main contributors*

This work has been carried out within the framework of the EUROfusion Consortium, funded by the European Union via the Euratom Research and Training Programme (Grant Agreement No 101052200 — EUROfusion). Views and opinions expressed are however those of the author(s) only and do not necessarily reflect those of the European Union or the European Commission. Neither the European Union nor the European Commission can be held responsible for them.

The main contributors

G. Cseh[2], Y. Feng[1], Y. Gao[1], M. Jakubowski[1], T. Kremeyer[1], S. Dräger[1], F. Reimold[1], M. Kriete[3], A. Pandey[1], G. Schlisio[1], G. Partesotti[1], V. Perseo[1], A. Alonso[4], Ch. Biedermann[1], S.A. Bozhenkov[1], Ch. Brandt[1], K.J. Brunner[1], R. Burhenn[1], B. Buttenschön[1], M. Endler[1], G. Fuchert[1], J. Geiger[1], R. Laube[1], L. Giannone[4], V. Haak[1], K.C. Hammond[6], M. Hirsch[1], J. Knauer[1], G. Kocsis[2], M. Krychowiak[1], R. König[1], D. Naujoks[1], M. Otte[1], F. Penzel[7], E. Pasch[1], A. Pavone[1], K. Rahbarnia[1], T. Szepesi[2], H. Thomsen[1], U. Wenzel[1], V. Winters[1] and the W7-X team

[1] *Max-Planck-Institut für Plasmaphysik, D-17491 Greifswald, Germany*

[2] *HUN-REN Centre for Energy Research, Konkoly-Thege út 29-33, 1121 Budapest, Hungary*

[3] *Auburn University, Auburn, AL, United States of America*

[4] *Laboratorio Nacional de Fusión. CIEMAT, 28040 Madrid, Spain*

[5] *Max-Planck-Institut für Plasmaphysik, Garching, Germany*

[6] *Princeton Plasma Physics Laboratory, Princeton, NJ, United States of America*

[7] *ITER Organization, CS 90 046, 13067 St. Paul Lez Durance Cedex, France*

Terminology & introduction

Detachment:

A promising plasma phase for future fusion reactor. Features:

- ❑ high radiated power due to intrinsic (from wall/target material) or seeded/injected impurity
- ❑ accompanied by reduction of particle flux and heat flux on the divertor targets (low-Z)

(hence protecting wall/target material from erosion)

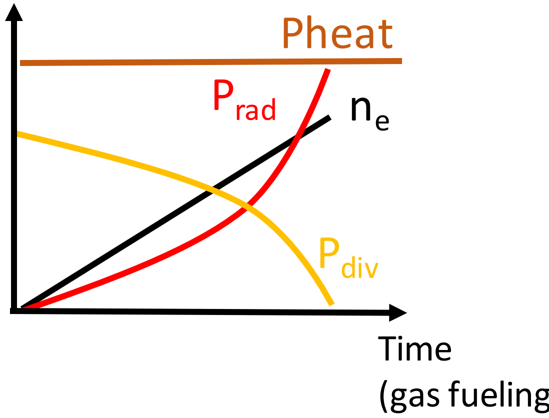

$$f_{rad} = P_{rad}/P_{heat} \sim 1$$

$$\Gamma_t \propto P_{heat}\,(1 - f_{rad})$$

$$\Gamma_t = \frac{P_{heat}\,(1 - f_{rad})}{(\gamma_t T_t + E_i)}$$

[Feng, NF,2021]

Preface:: terminology & introduction

Detachment:

A promising plasma phase for future fusion reactor

- ❑ high radiated power due to intrinsic (from wall/target material) or seeded/injected impurity
- ❑ accompanied by particle flux and heat flux reduction
  (hence protecting wall/target material from erosion

$$f_{rad} = P_{rad}/P_{heat} \sim 1$$

$$\Gamma_t = \frac{P_{heat}\,(1-f_{rad})}{(\gamma_t T_t + E_i)}$$

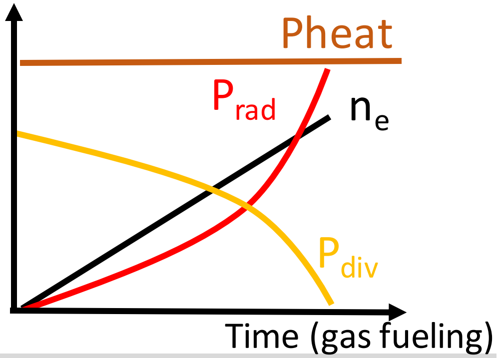

tokamaks (carbon device)

- radiation unstable (X-point (B_p=0); MARFE)

Processes accompanied:

Volume recombination (VR)

High recycling

Later, metal wall+N2&Ne-seeding

→ X-point radiation (XPR) within confined plasma

→ radiation stable & controllable

[Lipschultz, 1995,JNM]
[Stangeby,PPCF,2018]
[Krasheninnikov, JoPP,2017]
[Storht,NF,2022]
[Reimold,NF,2015]
[Bernert, NME,2017]

AUG

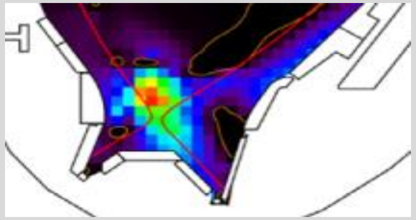

Stellarators (W7-X; carbon divertor targets)

- radiation stable (C and O impurity; +'standard' magnetic configuration)

! Instability in 'low-iota' plasma observed

[Zhang, PRL,2019]
[Schmits,2021,NF] [Jakubowski, NF, 2021]
[Feng, NF,2021]
[Winters,NF,2023]

- VR still under investigation

(observed in HDH w. ne~ 4×10^{20} m^{-3} in W7-AS)

- high recycling not seen

[Ramasubramanian, 2004 *NF]*
[Effenberg, NF,2019]
[Krychowiak, NME,2023]

Researching the role of N2&Ne-seeding & Detachment control are undergoing

! X-point radiation condensation is du to field expansion [Feng, NF, 2023]

XPR (due to carbon) features at W7-X are presented.

Overview of W7-X with key diagnostic locations - with 'standard' plasma

- 3D magnetic topology
- Five islands in the SOL (scrape-off layer)

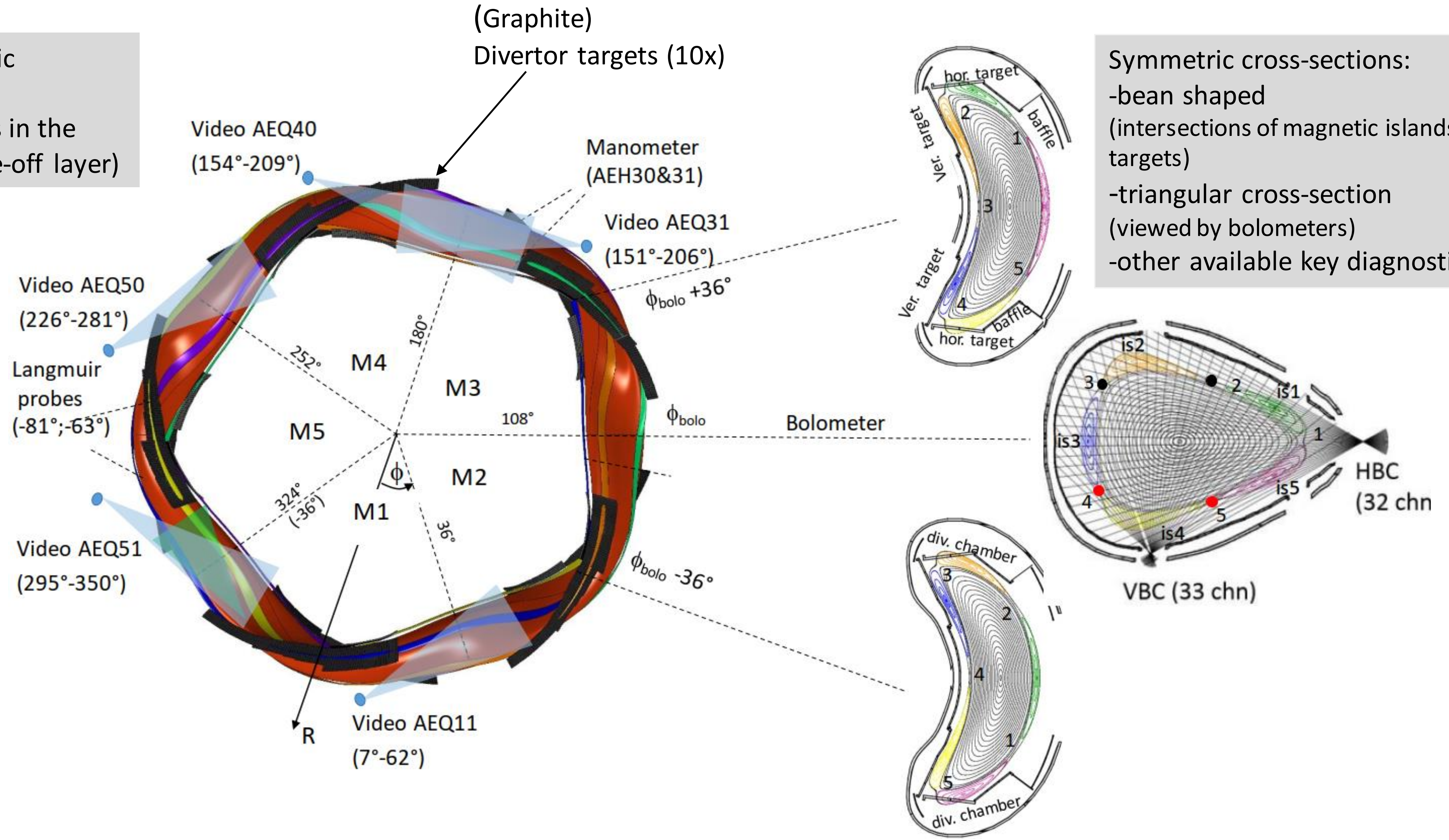

Symmetric cross-sections:
-bean shaped
(intersections of magnetic islands with targets)
-triangular cross-section
(viewed by bolometers)
-other available key diagnostics

OUTLINE

- ❑ **General observations of up/down asymmetry in density ramp experiment**
- ❑ **X-point radiation built-up and its asymmetric structure**
- ❑ **Examination of reversed field experiments**
- ❑ **Exploration of the mechanisms driving radiation asymmetry**
  - The simplified model of the ExB drift (with emphasis on poloidal drift) on impurity ion transport
- ❑ **Summary**

General observations: ‘standard’ configuration; ECRH plasma in OP1.2a

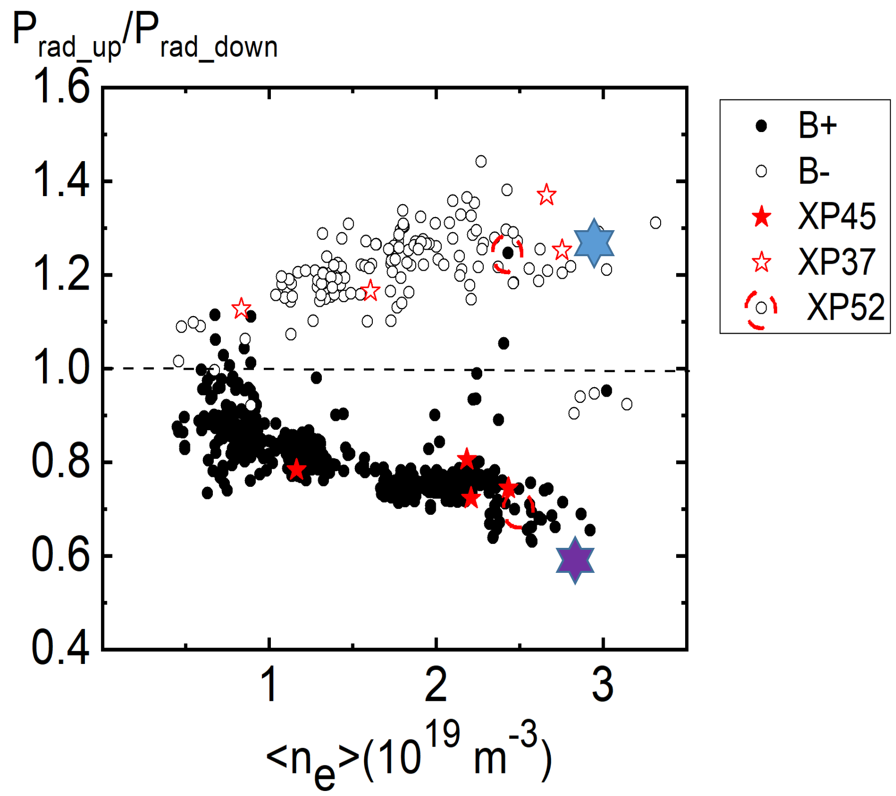

The two-camera bolometer system:

- FoV with up/down symmetric magnetic topology;
- HBC LoS constructed with up/down symmetry;

- 2D radiation distribution using bolometer tomography

[D. Zhang, et al 2021, NF]

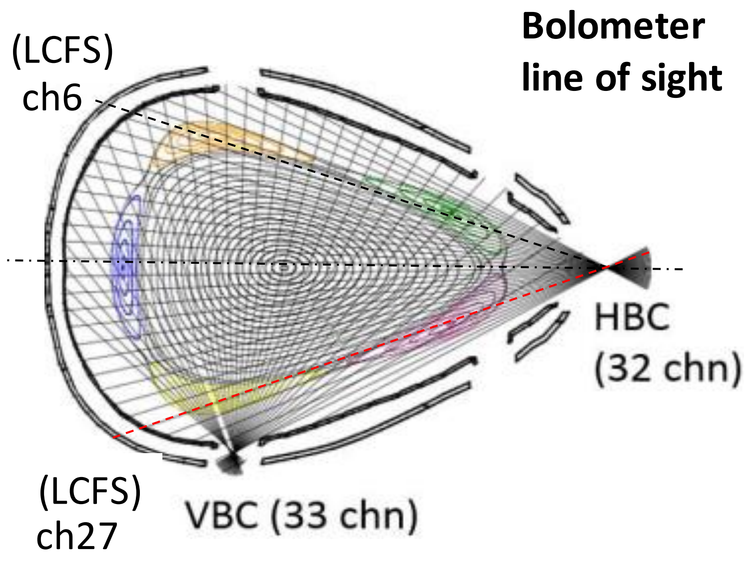

OP1.2a (O-impurity)

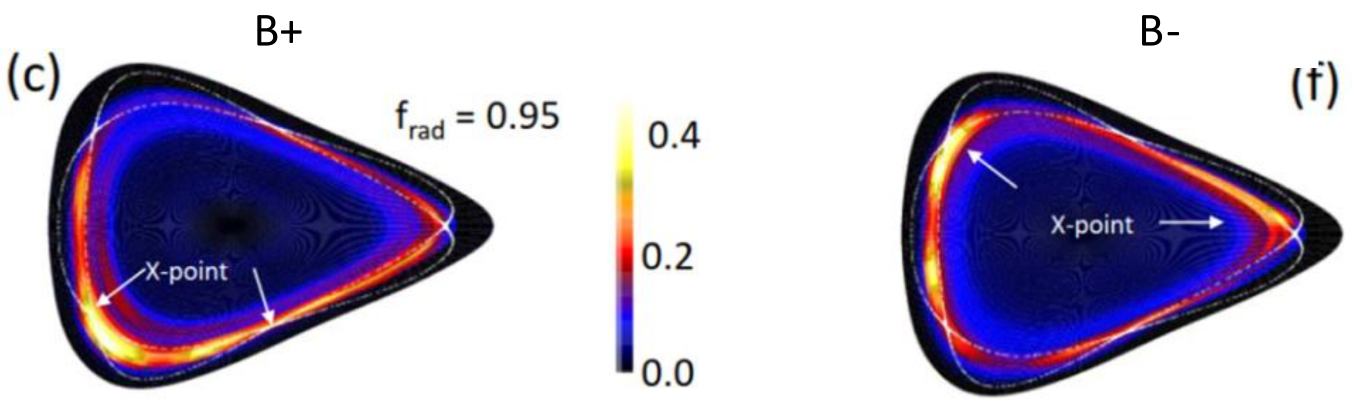

General observations in the plasmas after wall-boronization (OP1.2b)

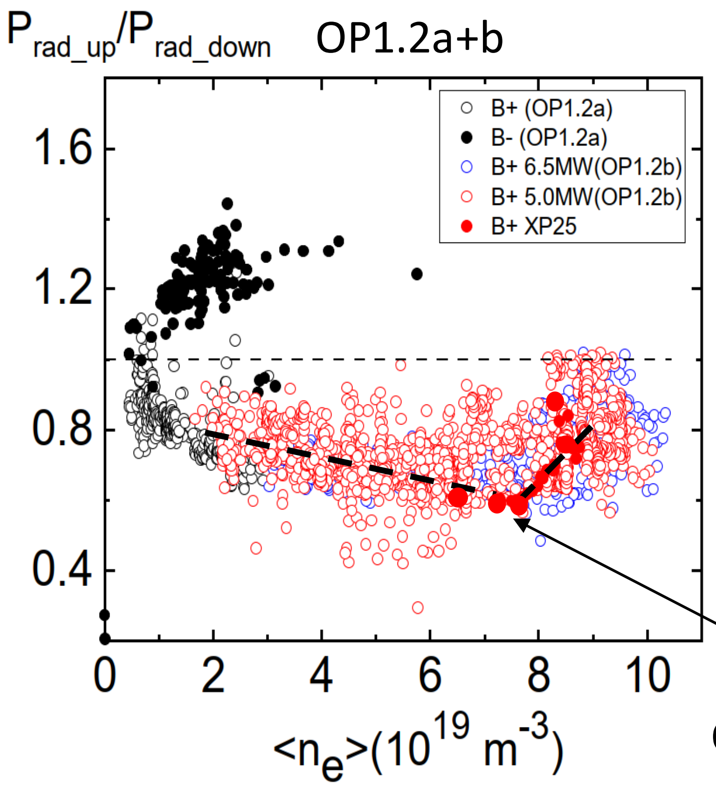

An example

Post-boronization
(C-radiation)

Onset detachment

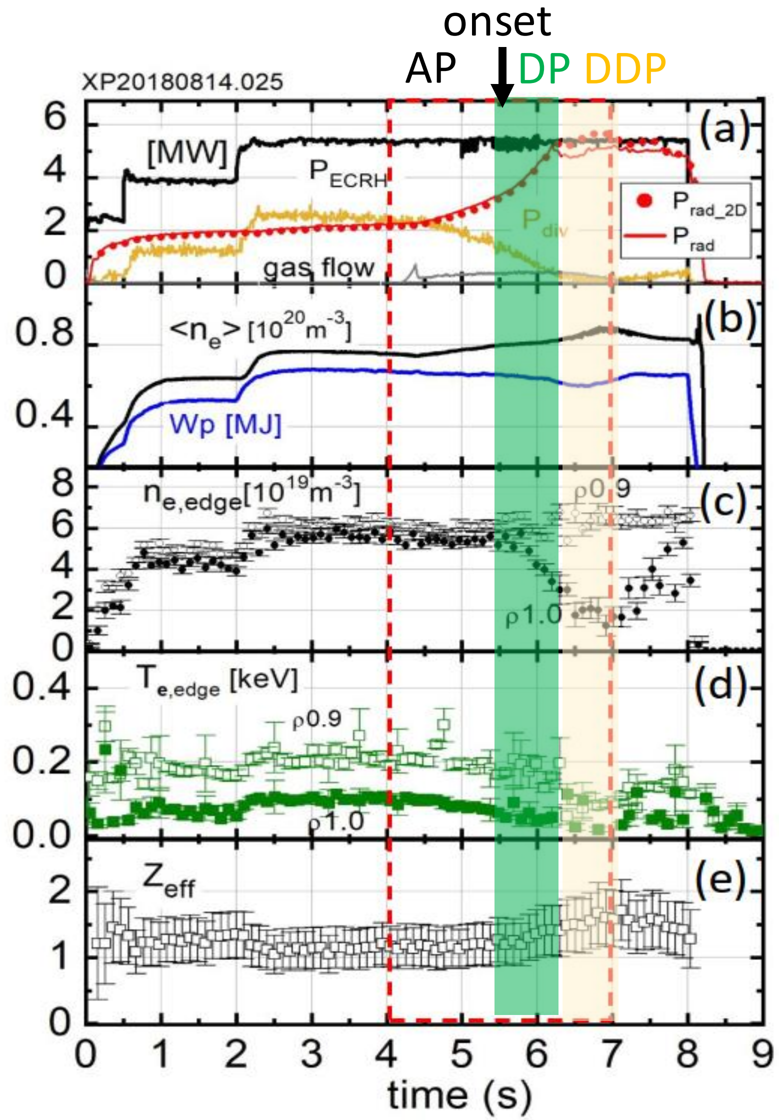

AP=attached plasma
DP=detached plasma
DDP=deeply detached plasma

Prad increasing
Pdiv decreasing

Density increasing

Edge density drops
(t>5.5s; onset DP)

Te(LCFS) drop from
100eV to <50eV

Zeff slightly increasing
(1.1→1.5)

➢ High-radiation regime → signaling plasma detachment

The edge plasma parameters and the up/down asymmetry

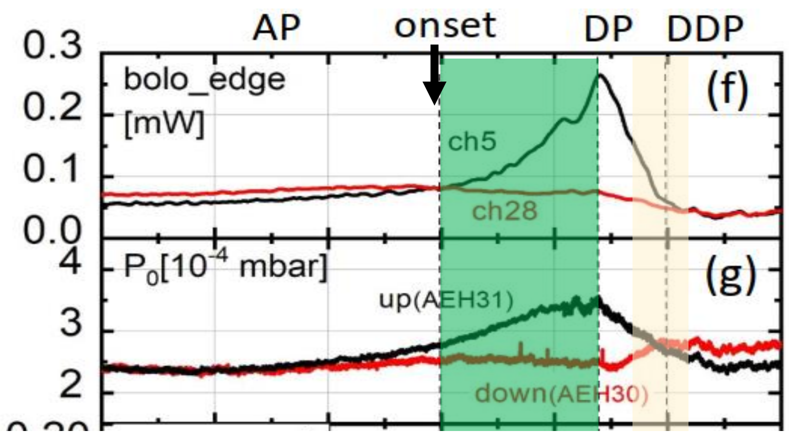

Bolometer edge signal:
Upper SOL radiation increasing
Lower SOL radiation flat

Neutral gas pressure P0:
Upper P0 increasing
Lower P0 flat

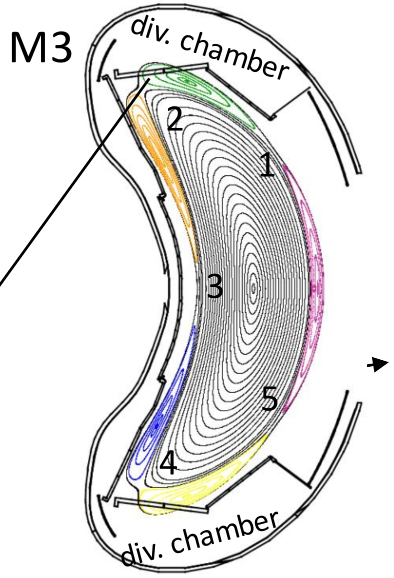

Neutral Pressure Gauges
(AEH31 vs AEH31
→ P0_up vs P0_down)

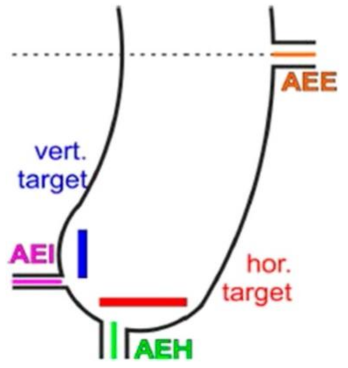

[Wenzel, 2019, RSI]

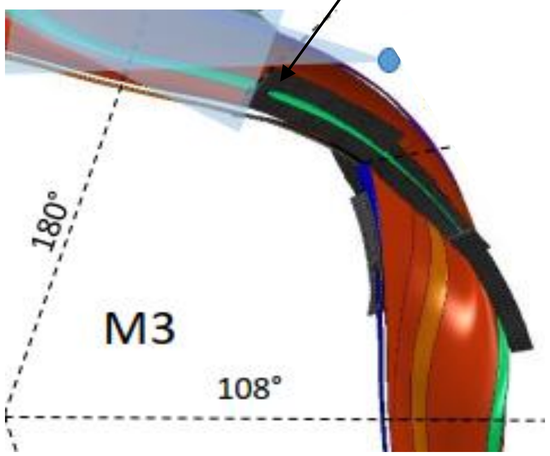

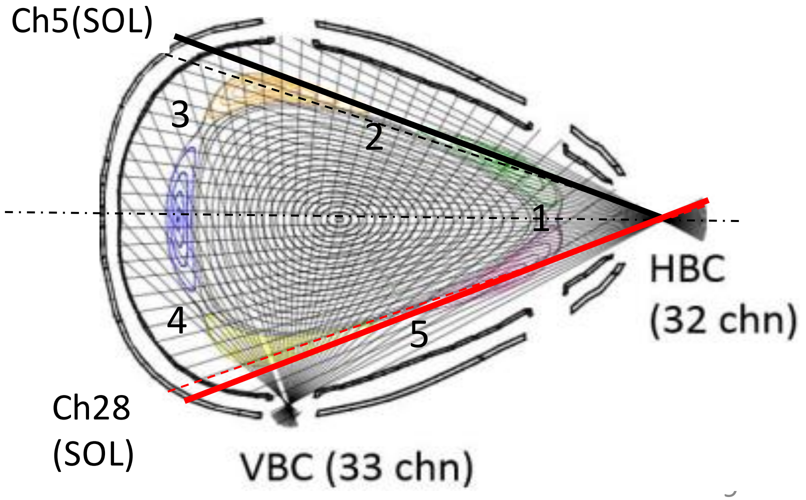

- ✓ Upstream radiative cooling→
lowering downstream Te,SOL→
Increasing neutral penetration length

The edge plasma parameters and indications of up/down asymmetry

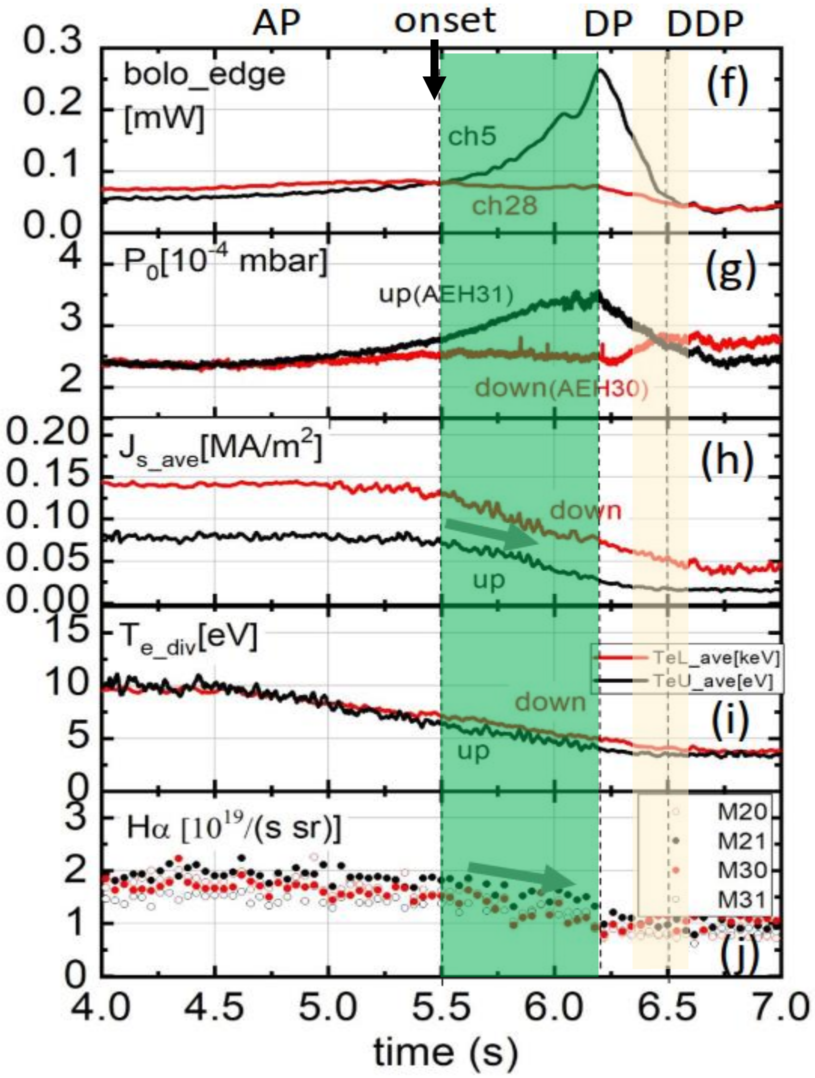

[Rudischhauser, RSI,2020]

[Kremeyer, NF,2022]

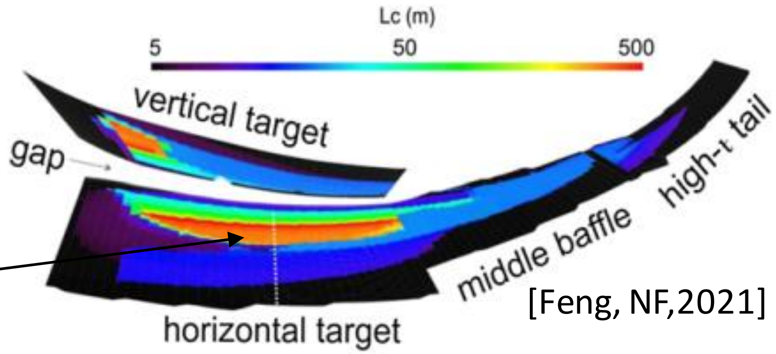

[Feng, NF,2021]

Langmuir probe arrays:

particle flux reduction

(definition of detachment onset)

Target temperature
reduces from 10eV →<5eV

Divertor visible light cameras

Hα signal decrease
(neutral recycling low)

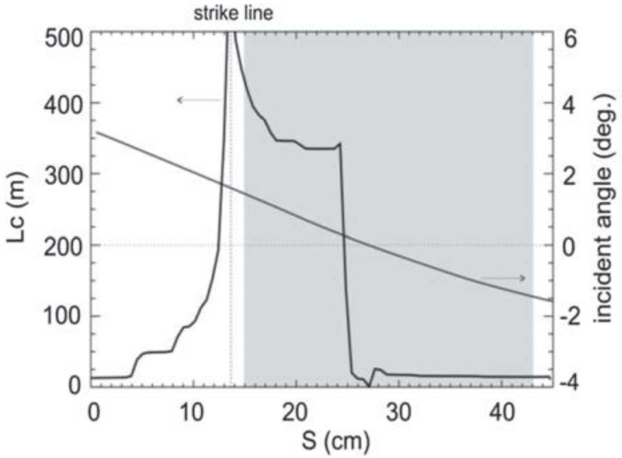

- General observations of up/down asymmetry in density ramp experiment

- **X-point radiation built-up and its asymmetric structure**

Chord-brightness evolution with plasma density and frad

Horizontal bolometer camera

Vertical bolometer camera

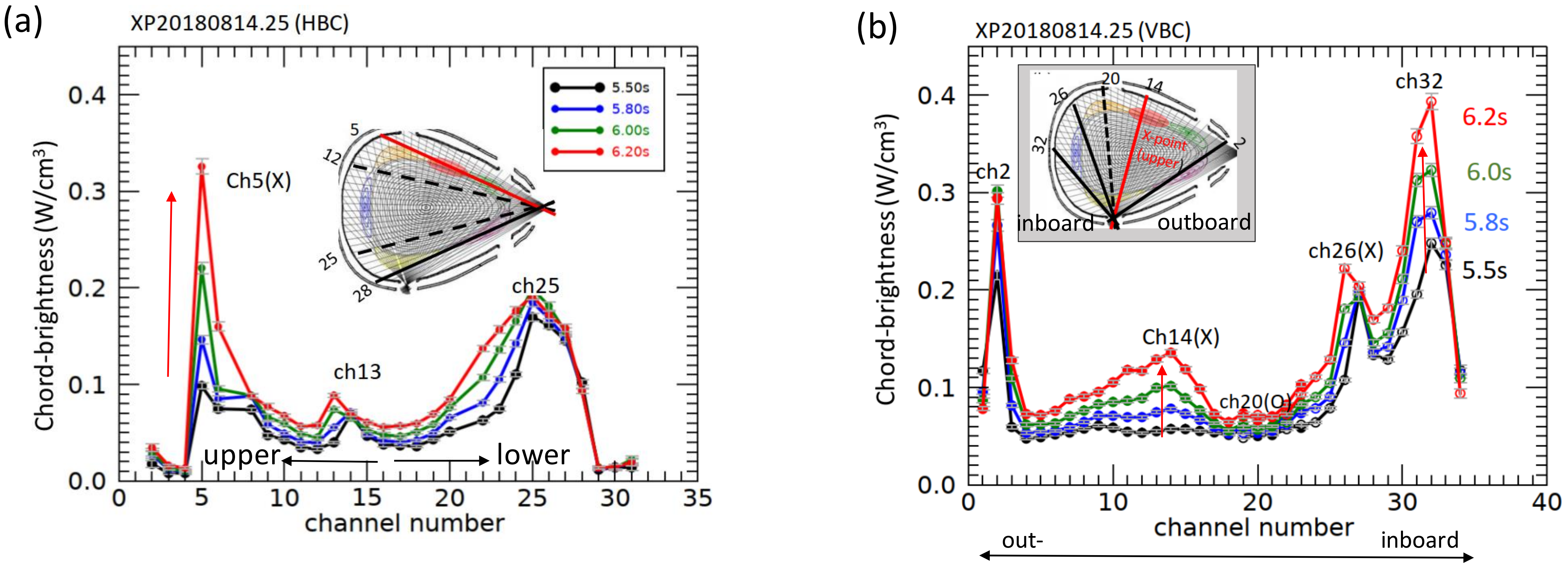

- Ch5 viewing upper SOL remarkable
- Its brightness rises with density

- Remarkable channels:

Ch14 viewing upper X-point and ch26,ch32 viewing inboard side

Chord-brightness evolution and the 2D radiation distributions

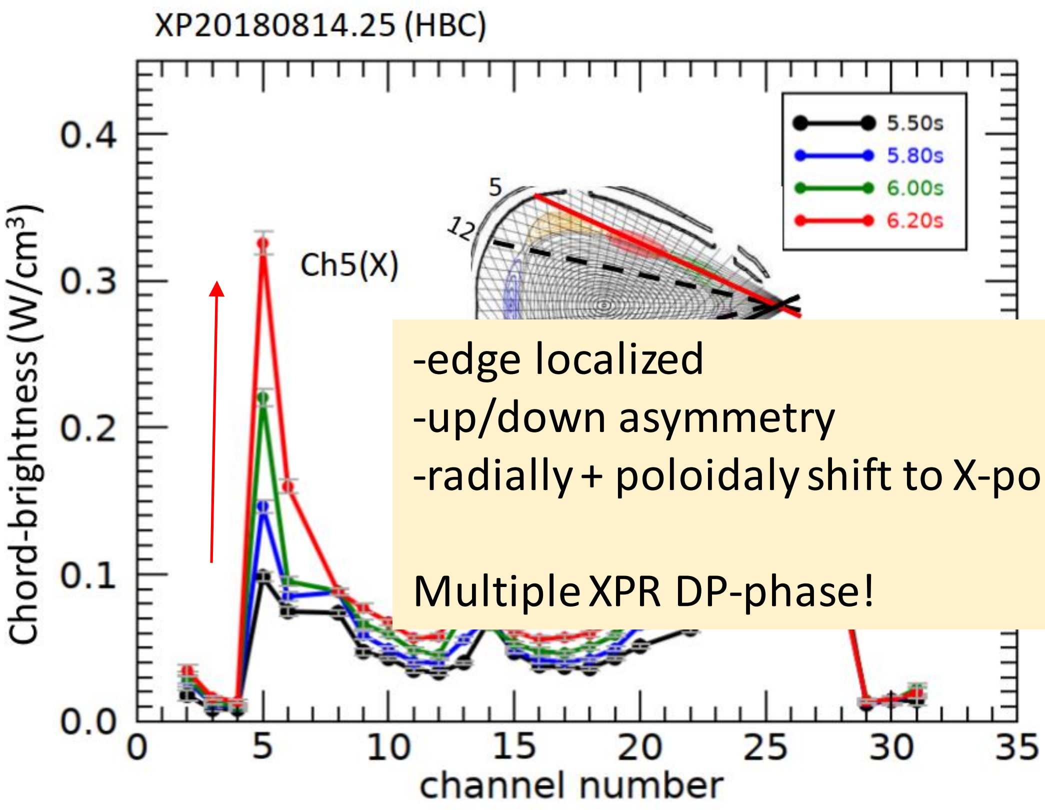

-edge localized
-up/down asymmetry
-radially + poloidaly shift to X-points

Multiple XPR DP-phase!

Bolometer tomography

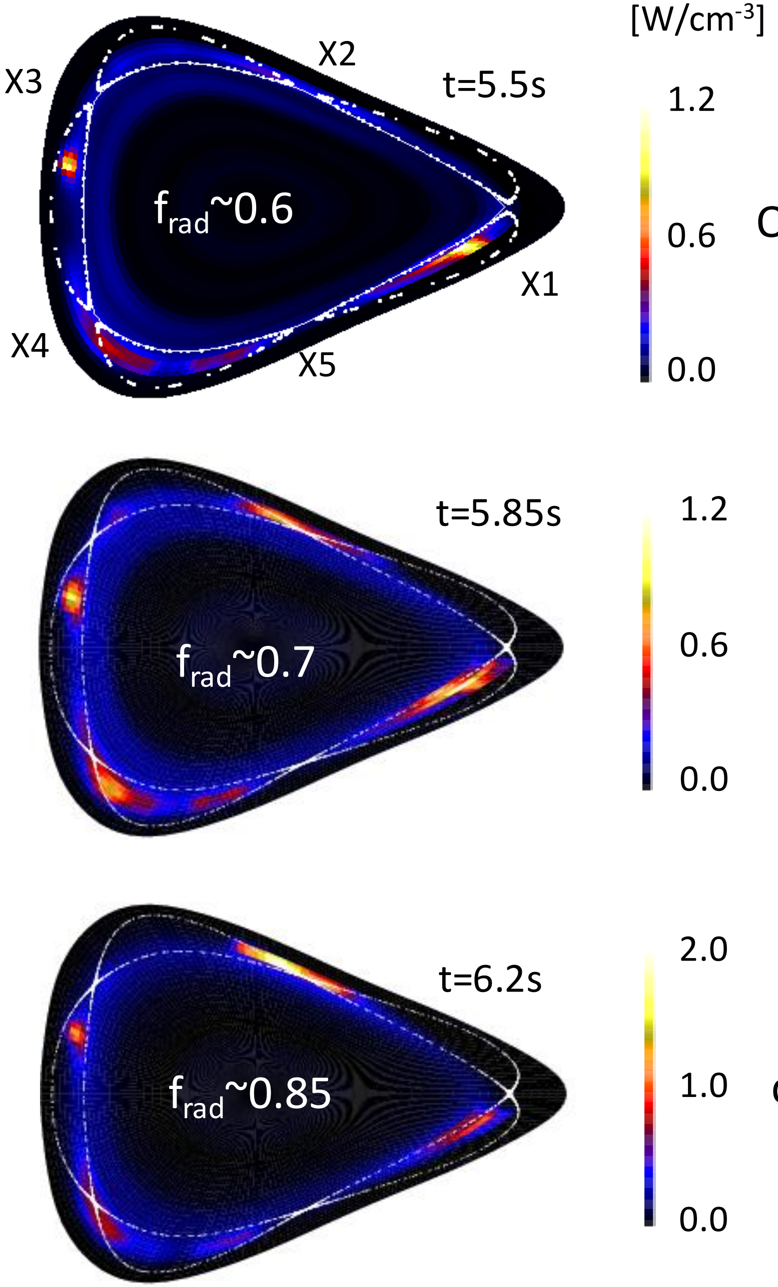

Onset detachment

detached (DP)

detached (DP)

Chord-brightness evolution with plasma density and frad
- transition from DP to DDP

XP20180814.25 (HBC)

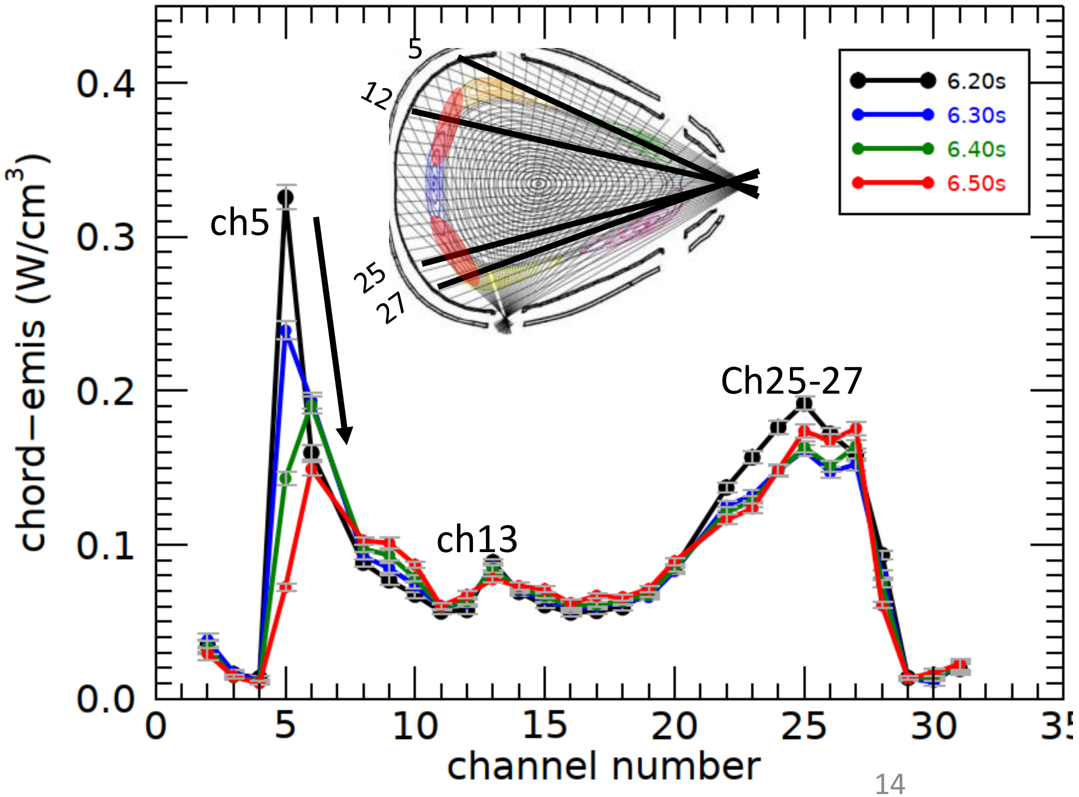

XP20180814.25 (VBC)

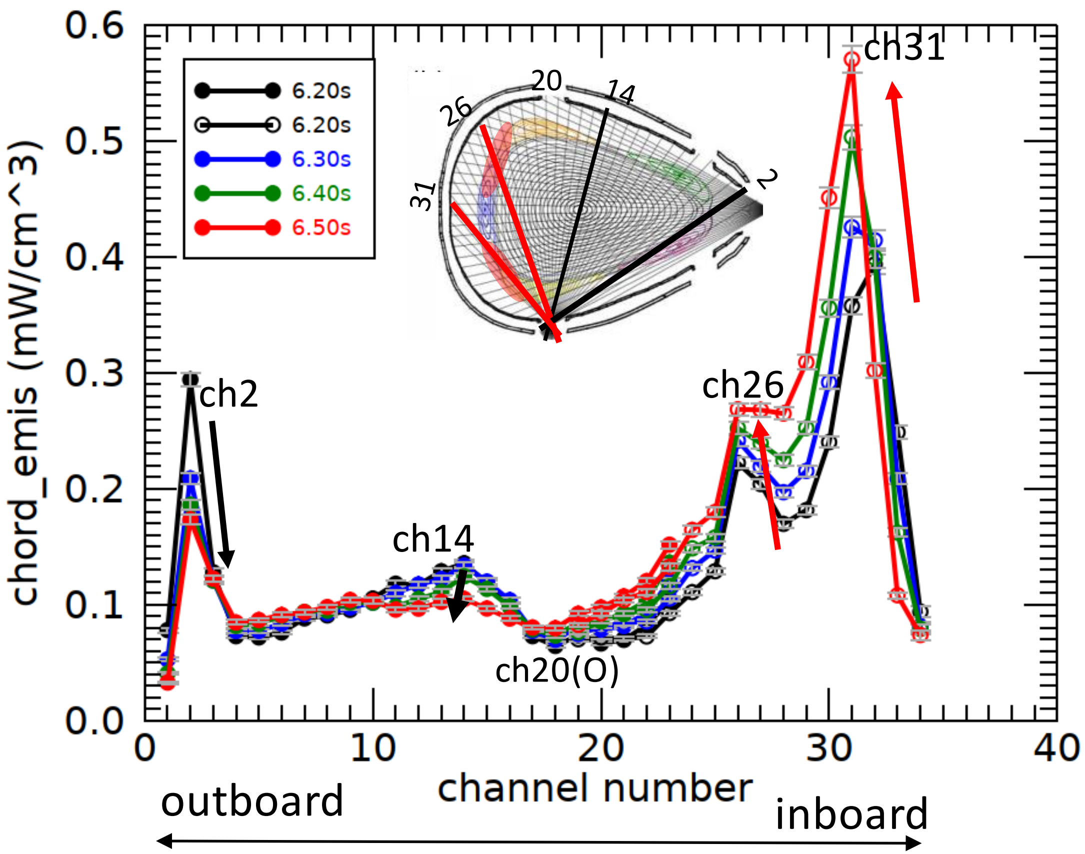

- Signal Ch5 in HBC decreases;
- The brightness in the upper SOL declines with density

- Signal Ch14 in VBC weakens;
- Signal Ch32 in VBC increases;
- The brightness's inboard side increase with density

Chord-brightness evolution and the 2D radiation distributions
- transition from DP to DDP

XP20180814.25 (HBC)

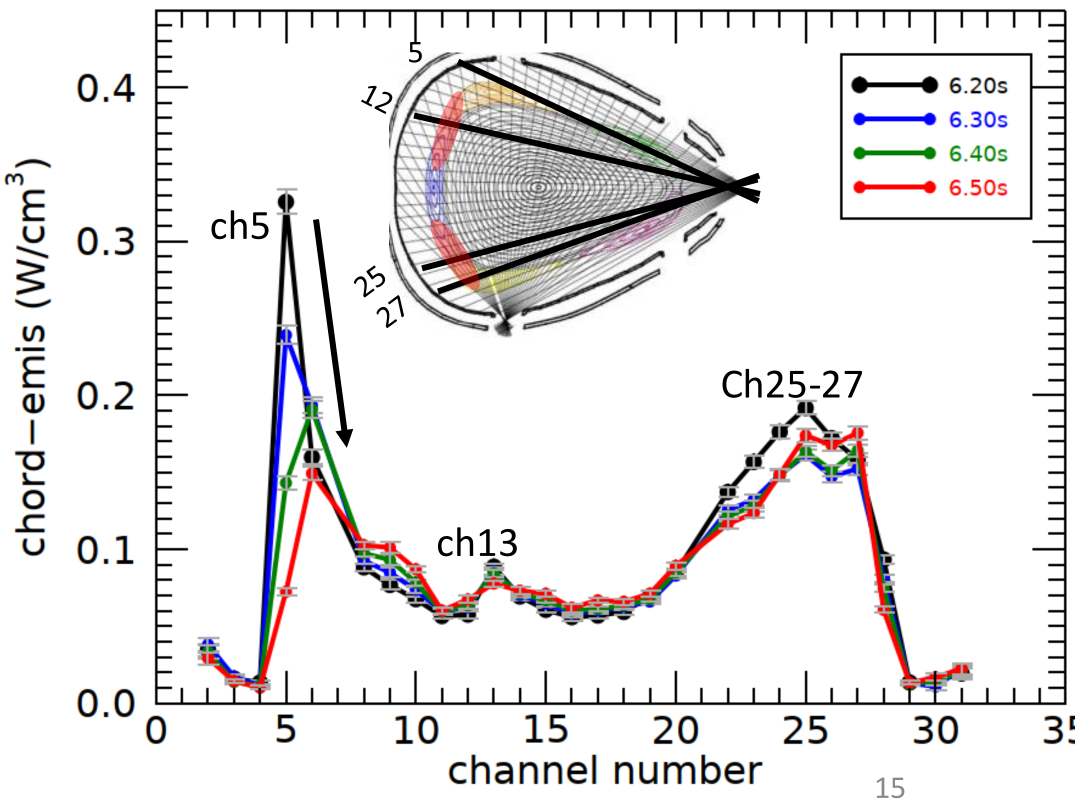

- Signal Ch5 in HBC decreases;
- The brightness in the upper SOL declines with density

Bolometer tomography

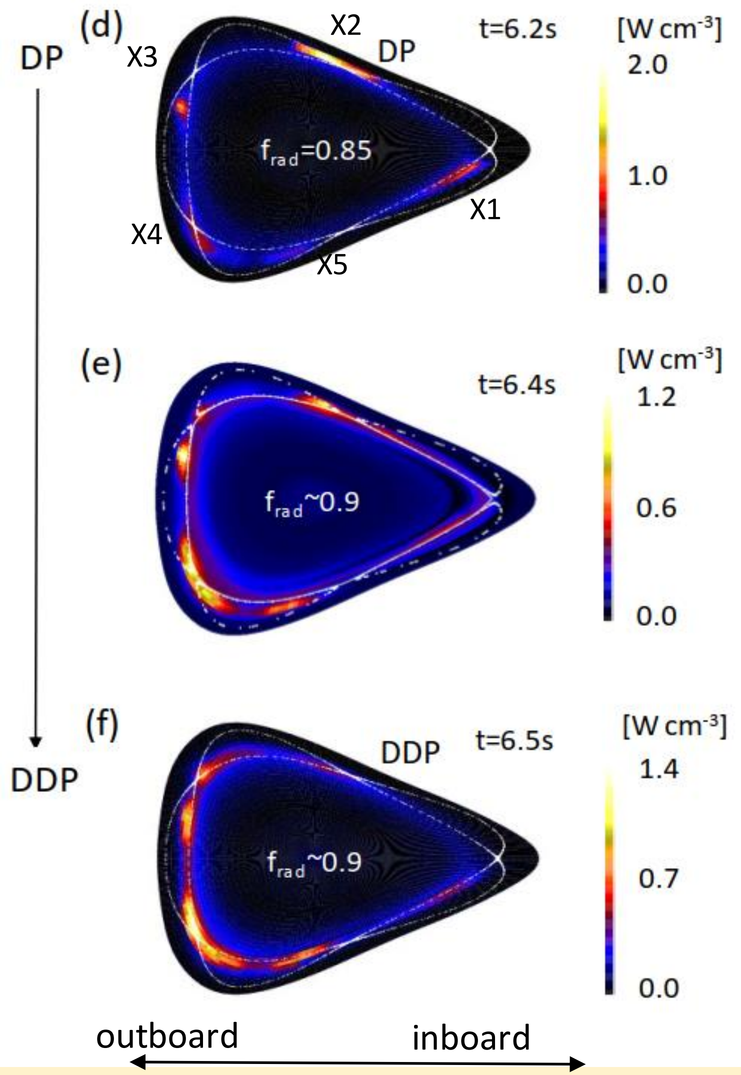

- Upper X-point radiation weakens;
- Intensive radiation appear at the inboard side (DDP)

Results derived from the 2D radiation patterns
- radiation zone radially inward shifting with frad

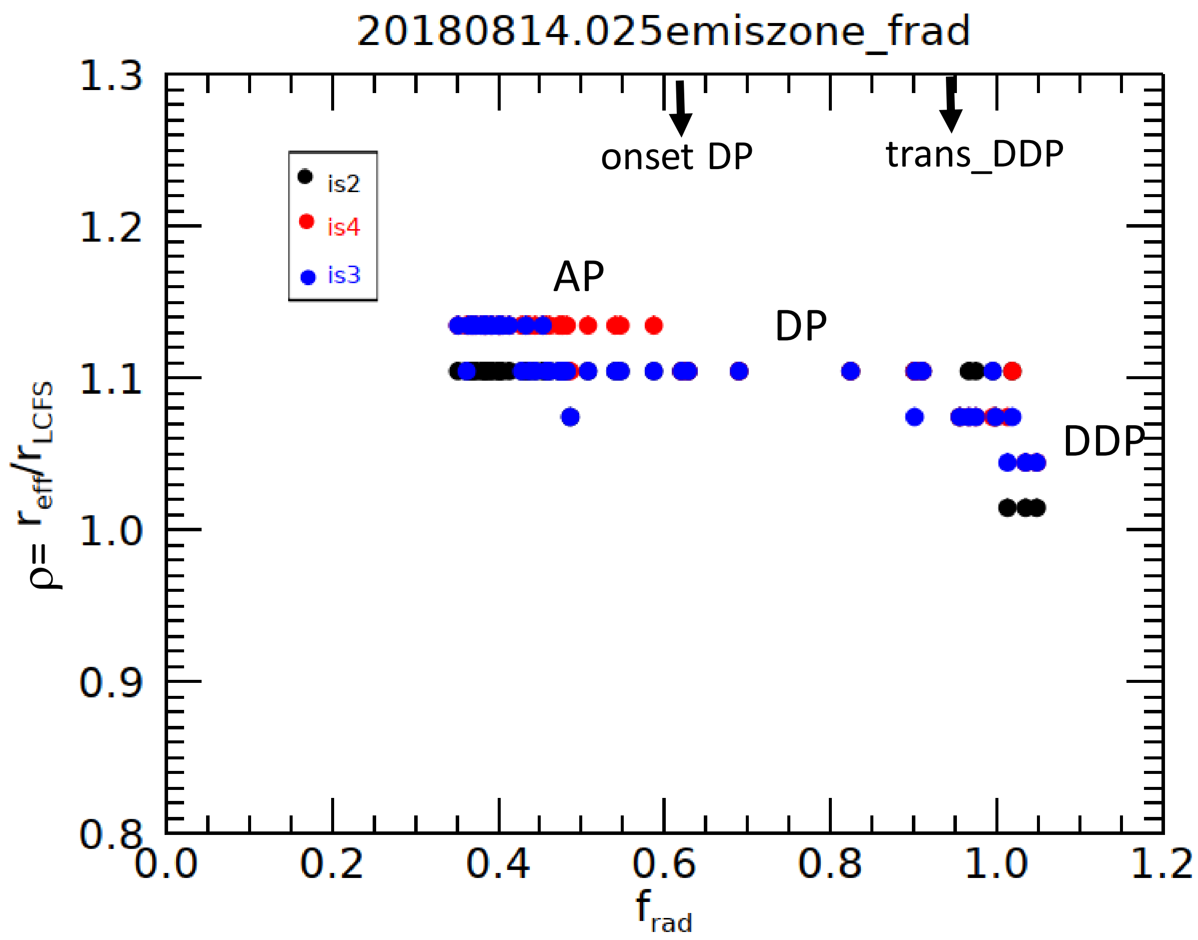

radial positions of the maximum emissivity in magnetic islands in is2, is3 and is4are analyzed;
It shifts from r/a=1.15 to ~1 as frad increases from 0.4 to unity.

Visible video camera observations support the bolometer results

AP phase (reference)

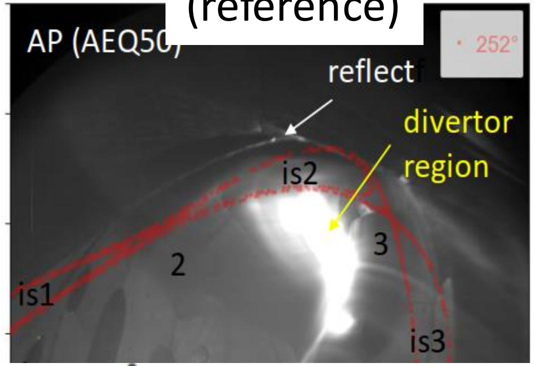

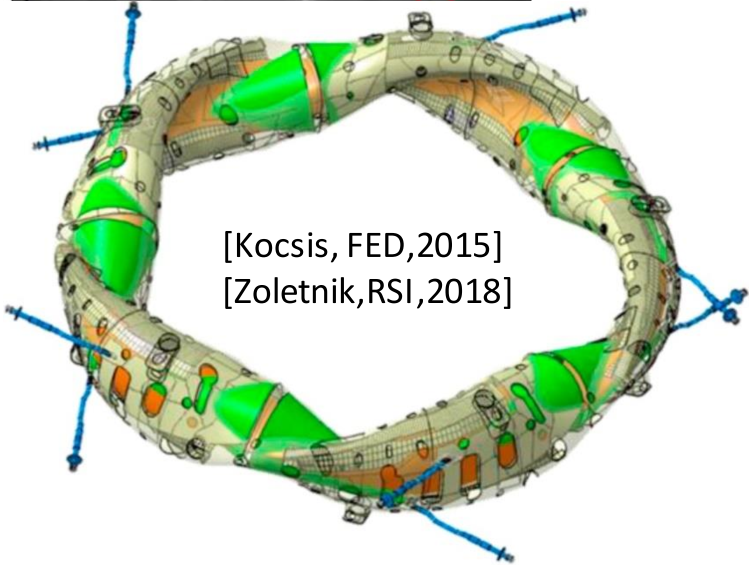

[Kocsis, FED,2015]
[Zoletnik,RSI,2018]

- Sensitive to visible light;
- E.g. from hydrogen, CII and CIII

Poincaré plots:
ϕ=247°
ϕ= 252°
(108°+2*72°)
ϕ= 257°

DP

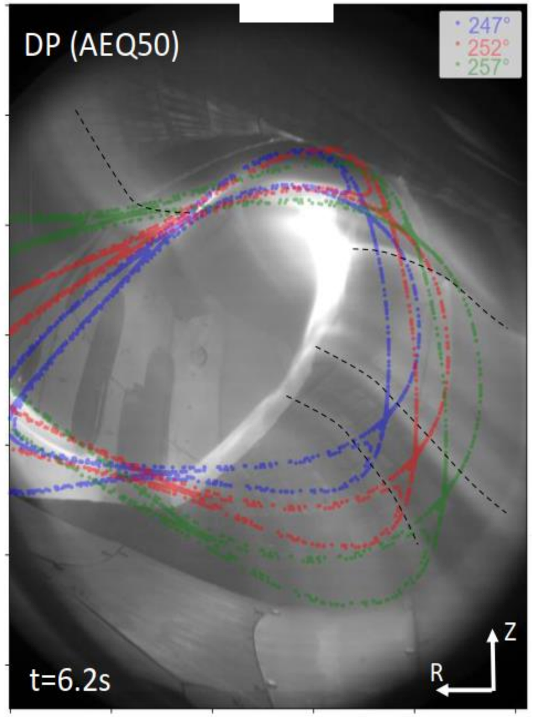

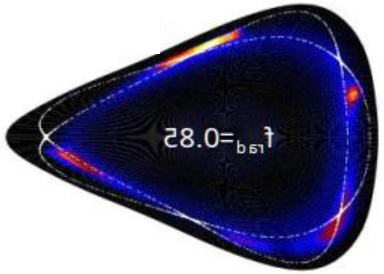

-stronger upper X-point radiator
-up/down asymmetry dominant

DDP

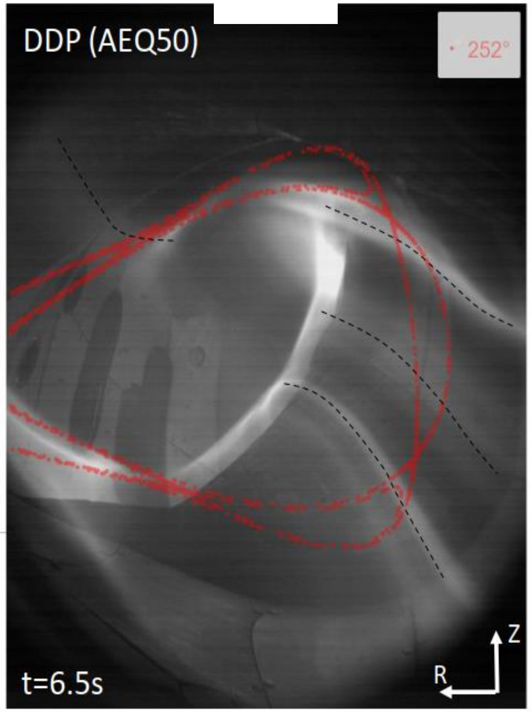

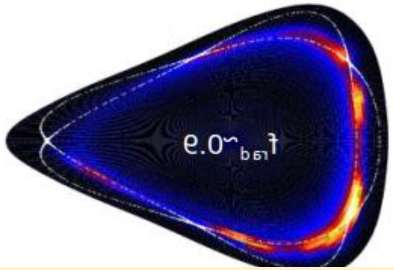

horizontally flipped

-upper X-point radiator weakens
-in/out asymmetry dominant

3D structure of the radiation belts from the visible video cameras - in the DP phase

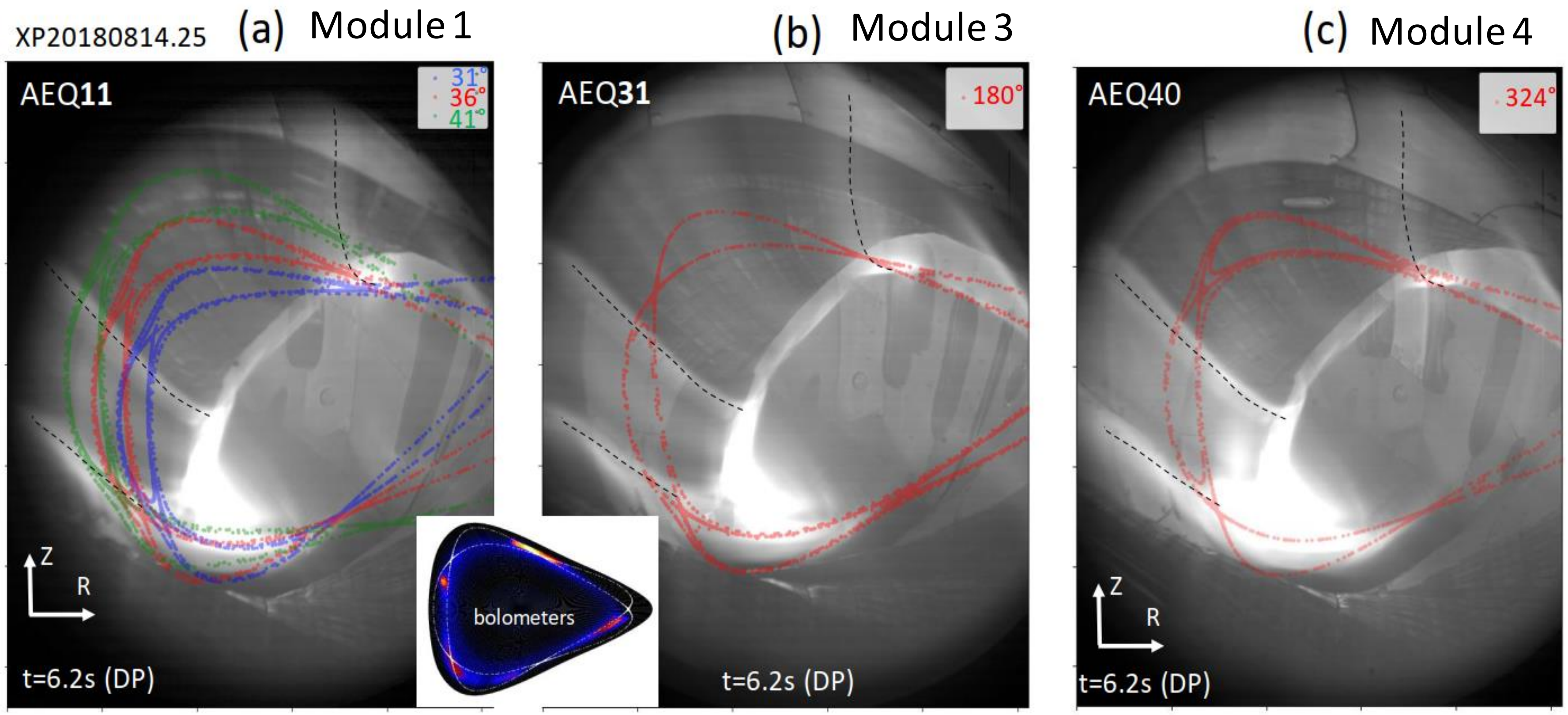

- Almost identical images in the four field periods (M1, M3, M4, and M5 (last slide))
- The X-point radiators appear at same poloidal position
- Radiation belts around three (of five) X-points
- These helical bands following the toroidal field period

Reversed field experiments in OP2.1 (2023)
-ECRH power step-down

! No density ramp programs

(a) **Normal B-field XP20230215.058**

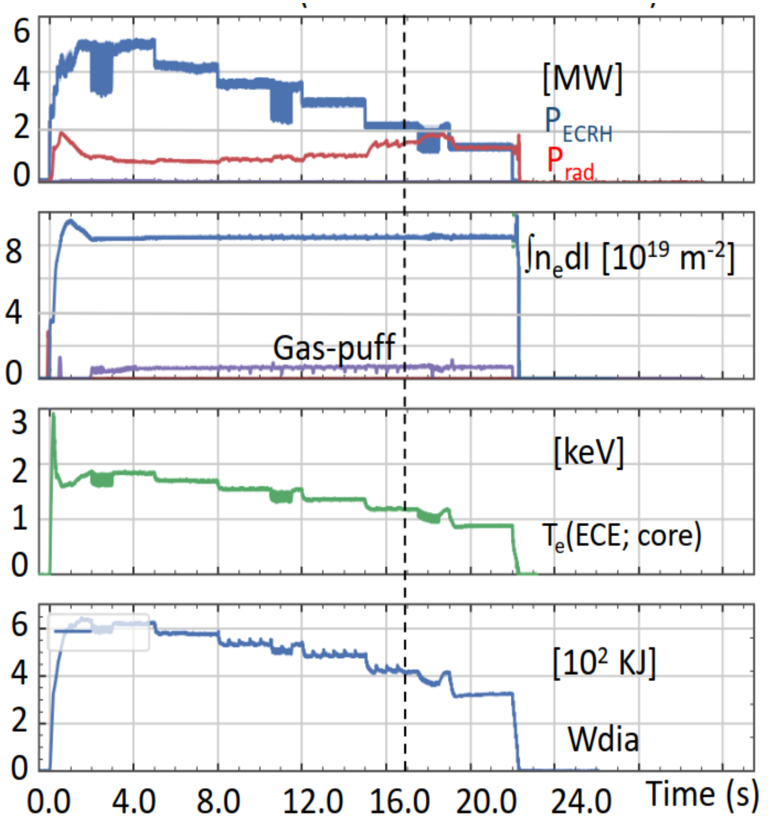

f_{rad}~0.7

Density not equal!

(b) **Reversed B-field XP20230117.074**

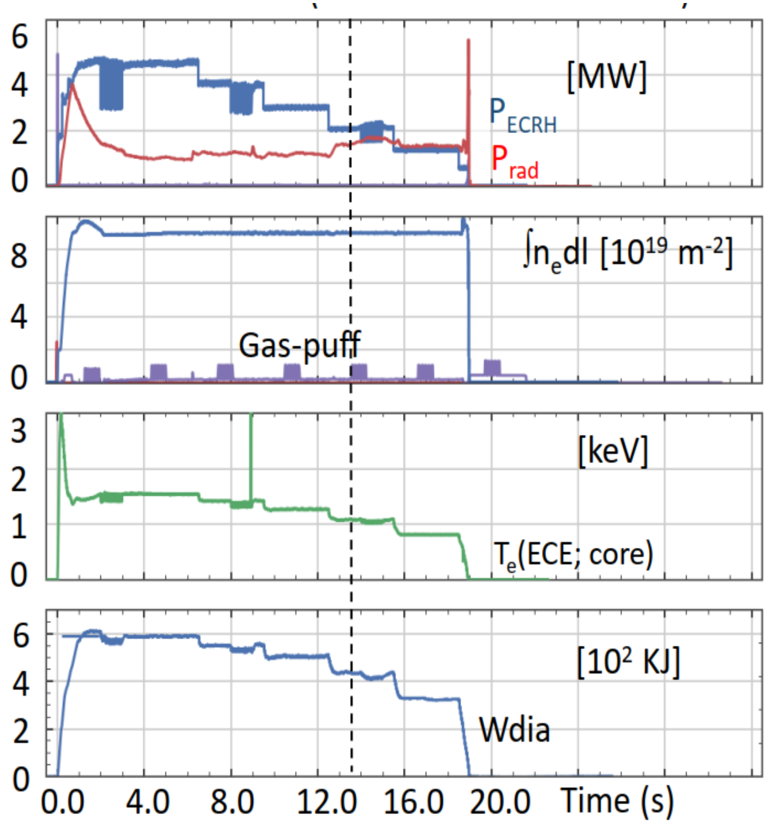

Reversed field experiments in OP2.1 (2023)
-Reverse asymmetry sign

! No density ramp prog

B+ case:
X4>X3
X2>X5
Is5>is1

B- case:
X4<X3
X2<X5
Is5<is1

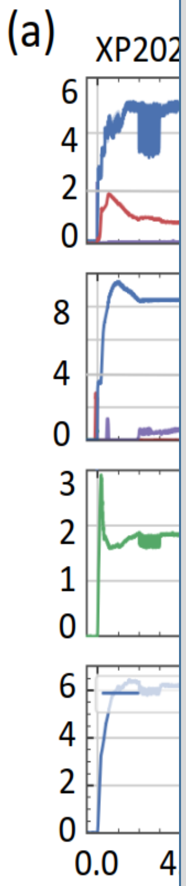

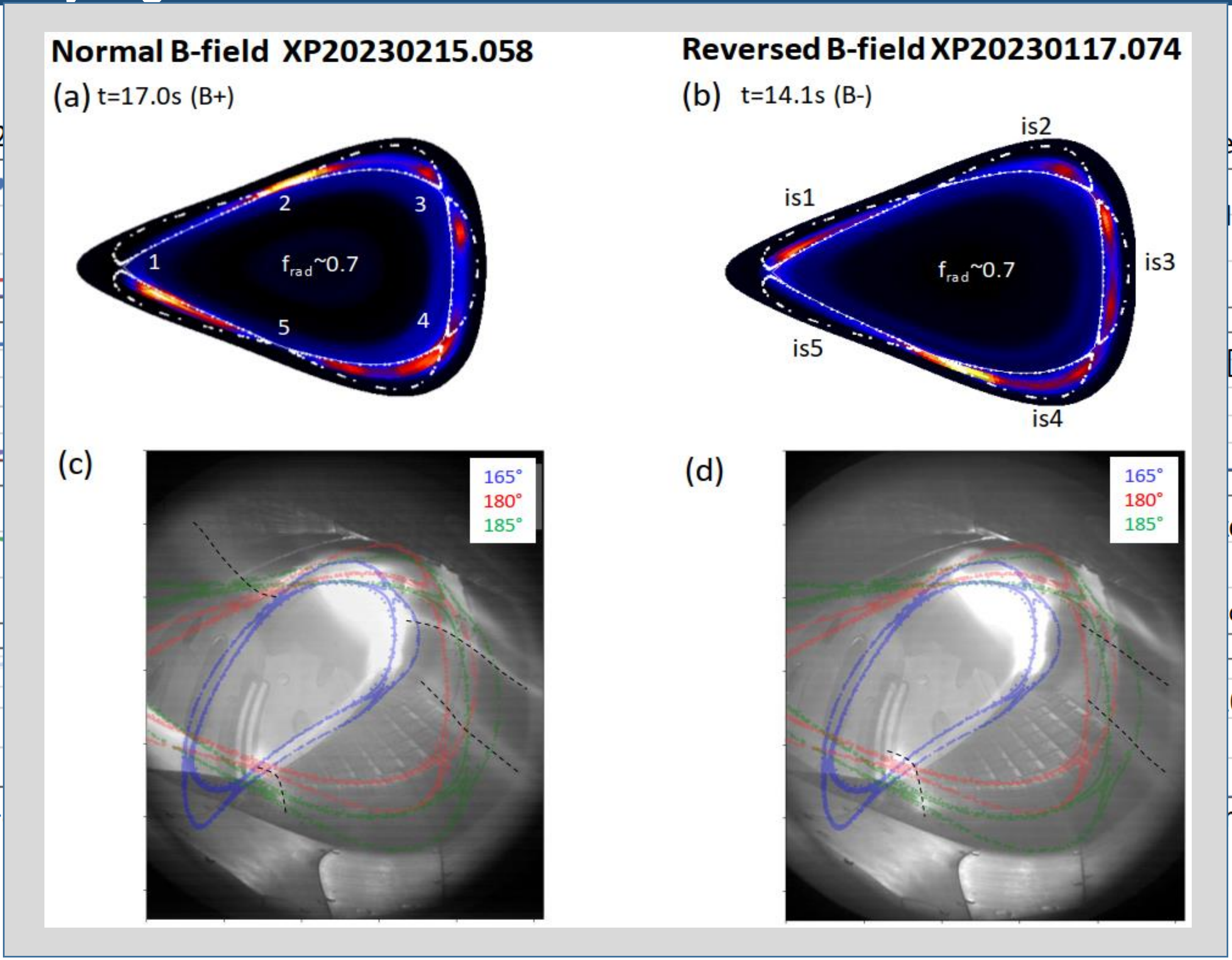

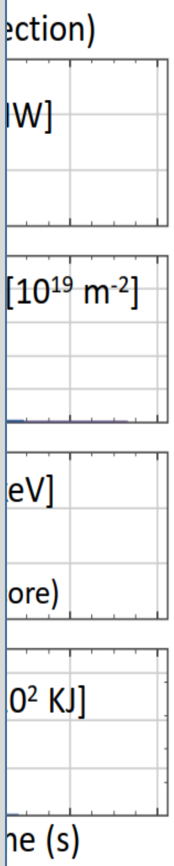

- General observations of up/down asymmetry in density ramp experiment

- X-point radiation built-up and its asymmetric structure

Exploration of the mechanisms driving radiation asymmetry: ExB drift

3D modeling results using EMC3-Eirene code w/o considering drifts

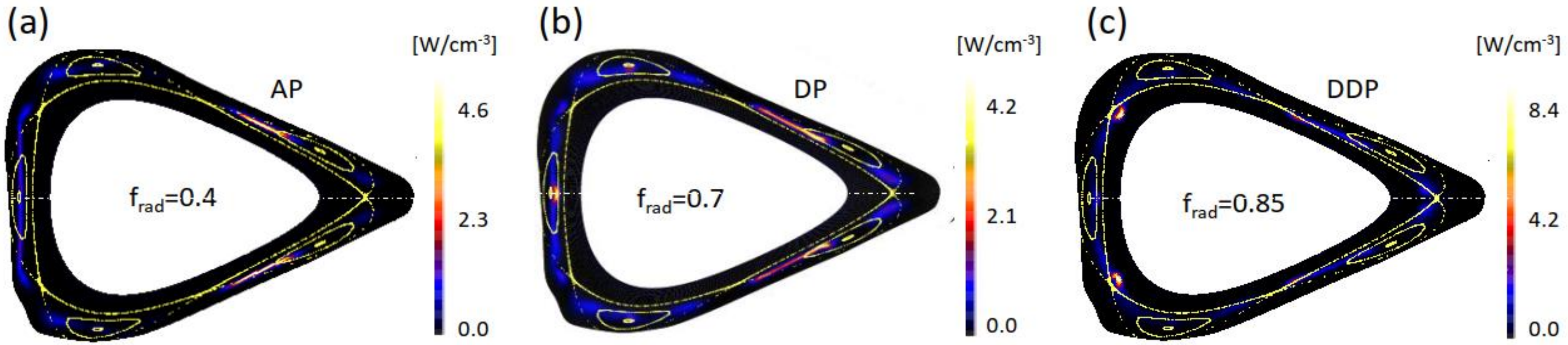

2D radiation distribution

$\varepsilon(r,\ \ ) = n_e n_z L_z(Z, T_e) \longrightarrow n_z(r, \theta) =?$ *source & transport*

Carbon transport
-from the source to the FoV of bolometers

- Wall-to-wall connection length Lc describes the averaged source distances;
- Lc~6m (near_TS) & 30m(far_TS)

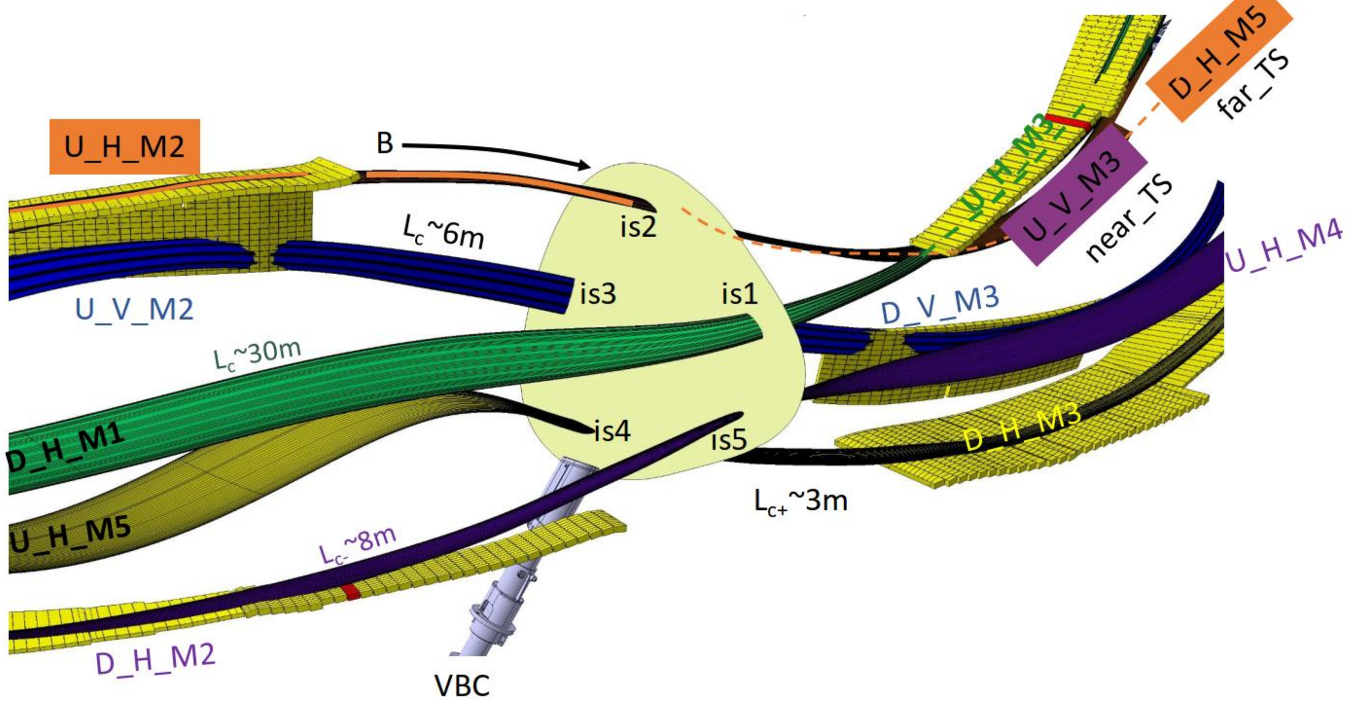

using EMC3-lite [Feng,2022,PPCF]

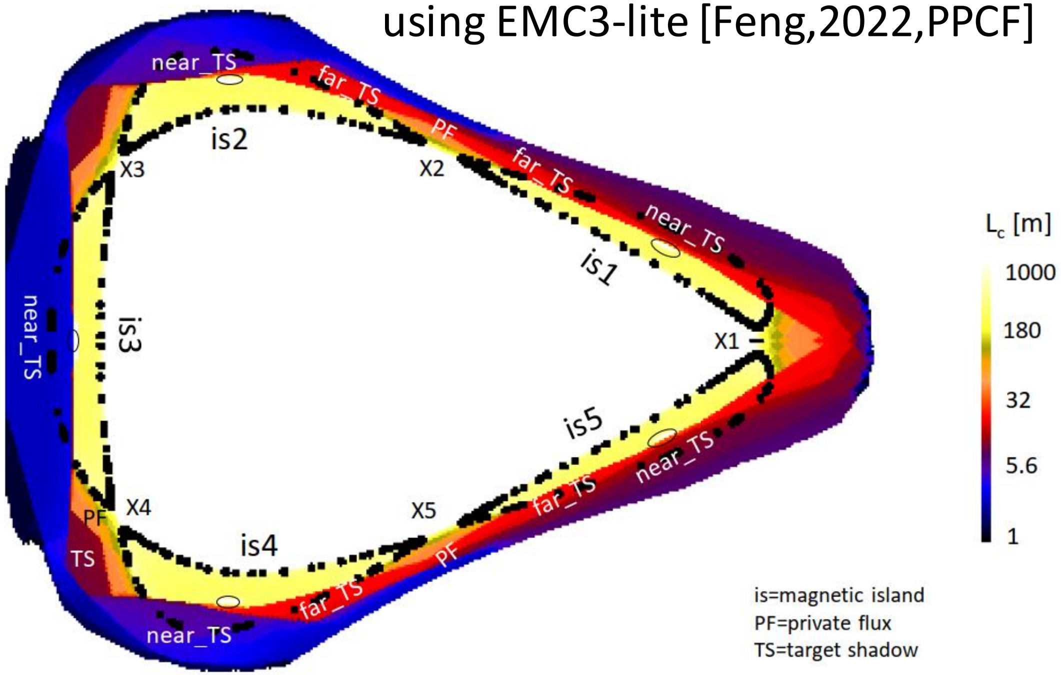

- Impurities released by PWI on the targets reach the triangular cross-section via //-transport and perpendicular transport;
- Parallel transport governed by impurity-ion frictions → impurity flow toward targets [Perseo et al 2019, NF]
- Cross field transport: diffusion + drifts

A simplified model of impurity transport in the island SOL
- friction dominant impurity flow

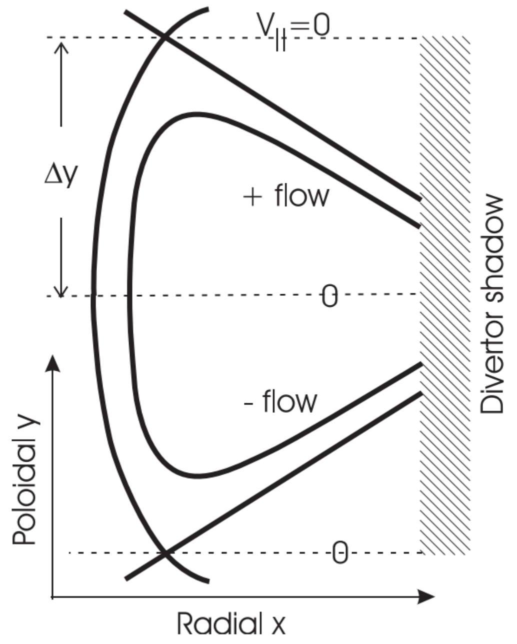

[Feng, NF, 2006]

Impurity parallel flow:

$$V_{Z\|} = V_{i\|} + \frac{\tau_{Zi} Z^2}{m_Z}\left(0.71\nabla_\| T_e + 2.2\nabla_\| T_i\right) + \frac{\tau_{Zi} Z e}{m_Z} E_\| - \frac{\tau_{Zi}}{n_Z m_Z}\nabla_\| T_i n_Z.$$

1D particle continuity equation in source free region:

Parallel transport:

Friction dominant impurity flow: Vz,f=$-\Theta V_{Z\|}$ (downstream, <0)

$$V_{Z\|} \approx V_{i\|}$$

Cross-field transport:

diffusive (D)

$$\frac{\mathrm{d}}{\mathrm{d}x}\left(\Theta V_{Z\|} n_\mathrm{I} - D\frac{\mathrm{d}n_\mathrm{I}}{\mathrm{d}x}\right) = 0, \quad (9)$$

$$n_\mathrm{Is} = n_\mathrm{Id}\exp\left(-\int\frac{\Theta V_{Z\|}}{D}\mathrm{d}x\right) \quad (10)$$

- Higher $\Theta V_{Z\|}$ causes low impurity density in the island SOL

Examining the classical drifts ExB
- considering the normal field direction

M. Kriete, NF,2023
K. Hammond, PPCF, 2019
Y. Feng, PPCF, 1998

Poloidal drift: $V_{d,\theta} \propto E_r x B$

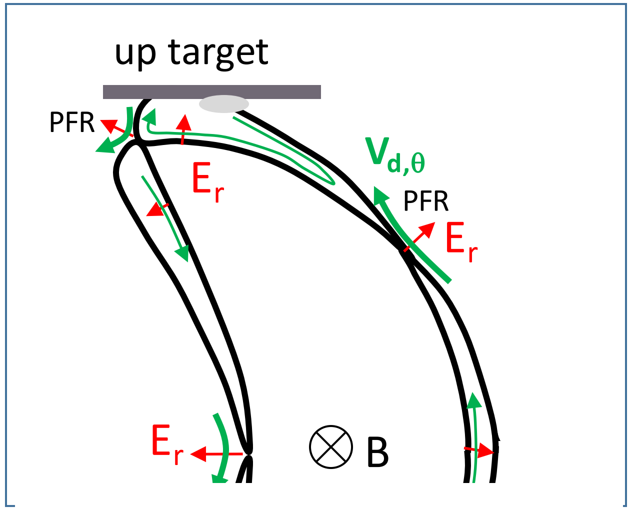

E_r direction:

- from higher-Te LCFS toward the lower-Te O-point within the islands;
- away from the LCFS in the PFR;
- The net pol. drift $V_{d,\theta}$ is anti-clockwise pointing towards down-target;

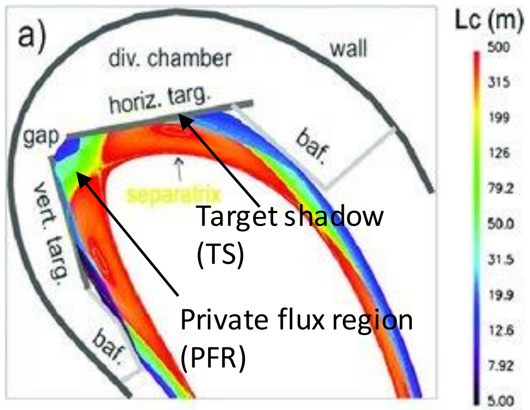

[Y. Feng, 2021,NF]

E x B poloidal drifts are more important than E x B radial drifts.
[Stangeby, NF, 1996]

Radial $V_{d,r} \propto E_\theta x B$

- Due to the potential drop along the B-field line from up- to downstream (i.e. E//-field)

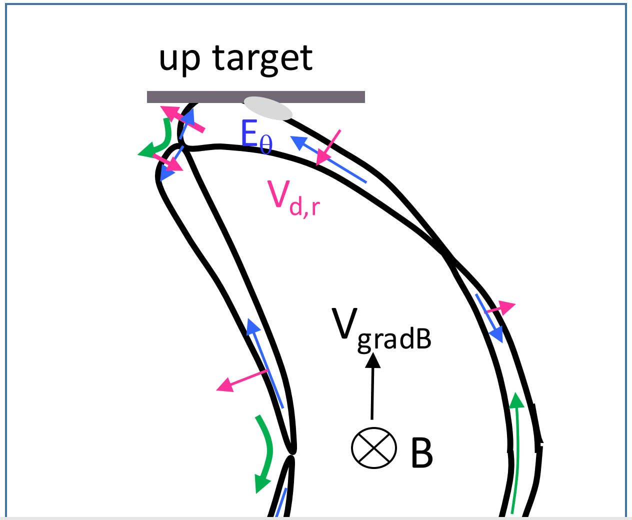

- $E\theta$ points from X-point (higher Te) toward target (lower Te) along the separatrix
- Vd,r points from island towards PFR or from PFR to the island.
- This part is ignored.

How about their impacts on impurity transport?

A simplified model of poloidal drift effect
- the effect on impurity transport in the island SOL

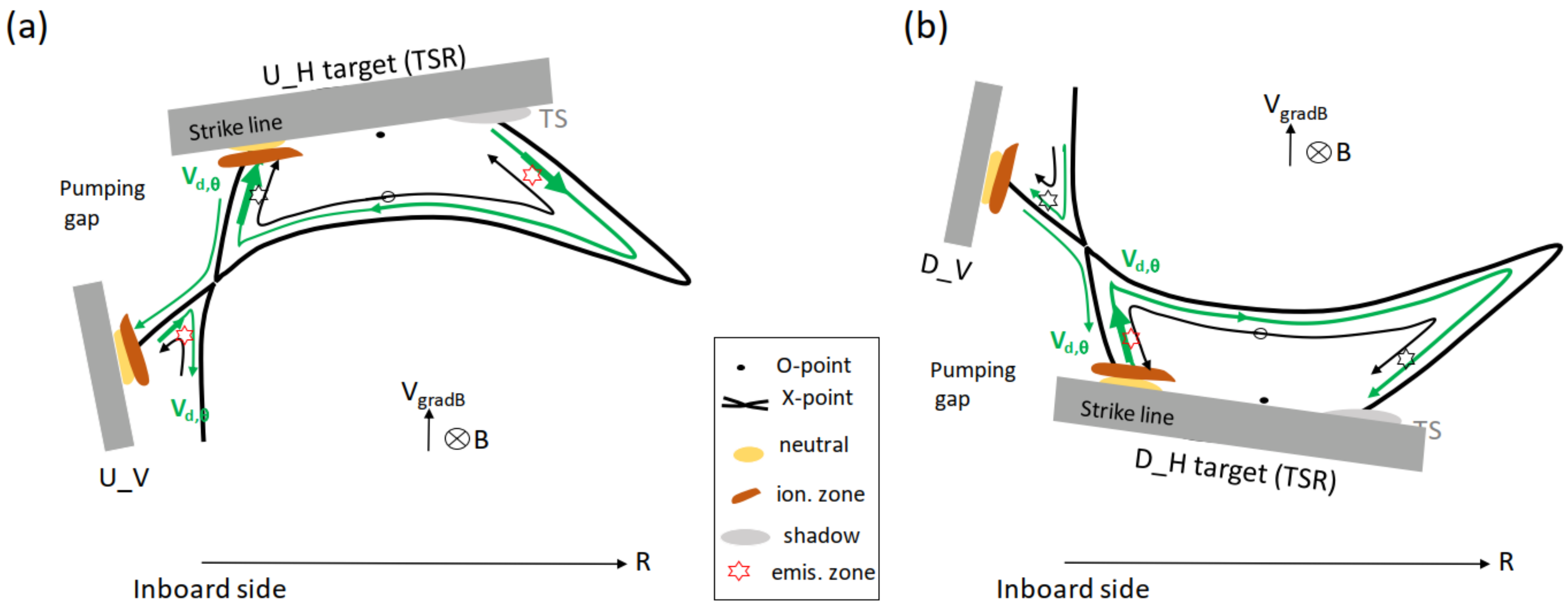

Considering poloidal drift Vd:

$$n_{IS}(xp) = n_{Id}\exp\left(\int_{\lambda_0}^{x_p}\frac{Vz,f + V_d}{D}\,dx\right)$$

- ✓ At ✡, Vd = $+V_{d,\theta}$ (>0, toward the LCFS)
- ✓ At ✡ Vd = $-V_{d,\theta}$ (<0, toward the target or TSR)

Up/down asymmetry of impurity (e.g. 'star' marked positions):

$$\boxed{\eta_{Is} \propto \eta_{Id}\exp\left(\int\frac{2\,V_{d,\theta}}{D}\,dx\right)}$$

η_{Id}: source asymmetry (at down stream TS)

❑ Upstream drift → higher impurity density → higher radiation

Explanations of impurity radiation asymmetry in the triangular cross-section: upper island is2 vs lower island is4

Model

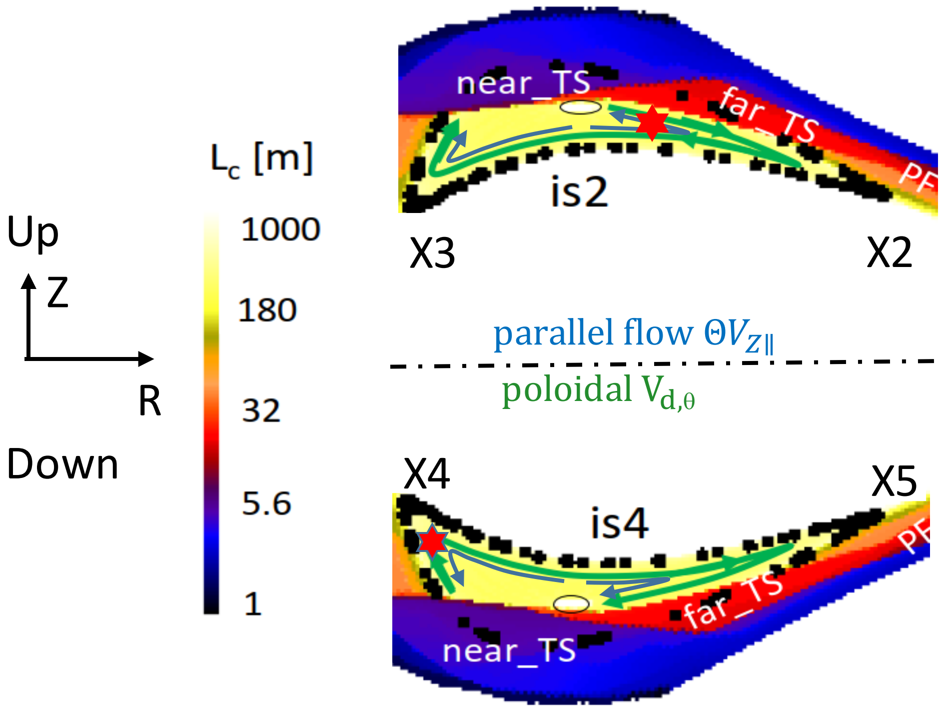

Bolometer tomography

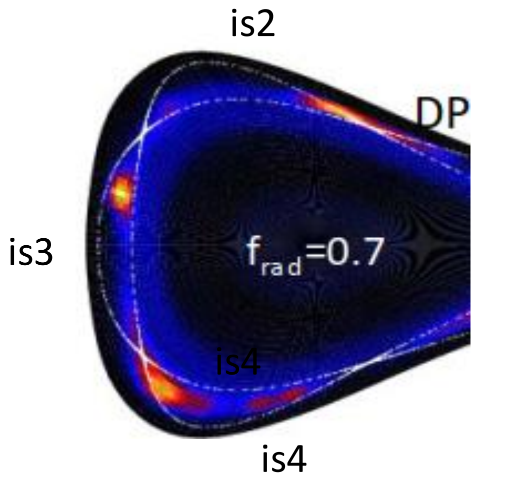

- ❑ Higher impurity radiation:
  - ✓ In IS2, in the right partition
  - ✓ In IS4, in the left partition
  - → Corresponding to regions with upstream pol. **E**x**B** drift

Explanations of impurity radiation asymmetry in the triangular cross-section: within the magnetic island is3

Model

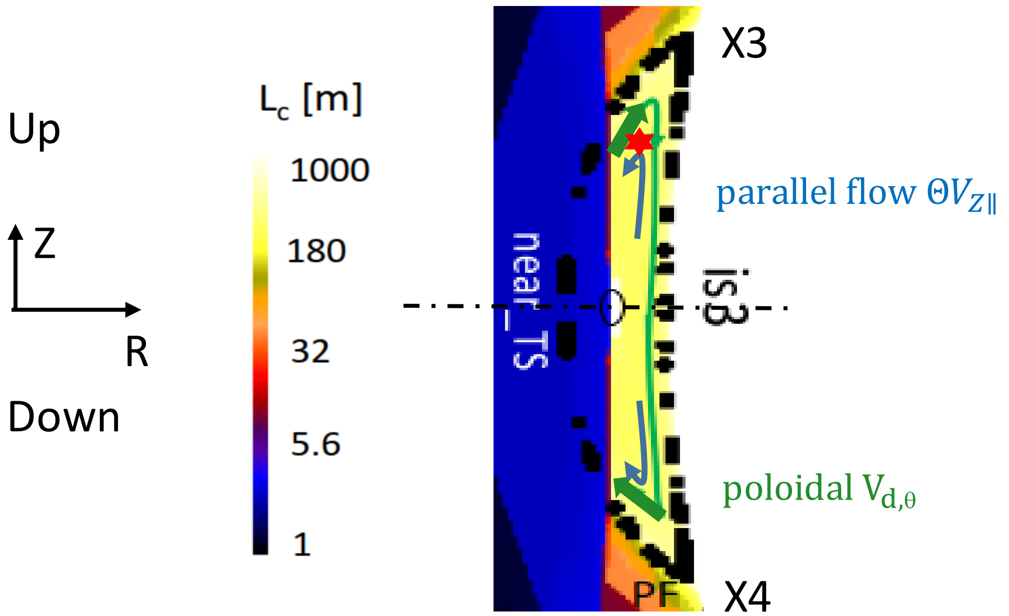

Bolometer tomography

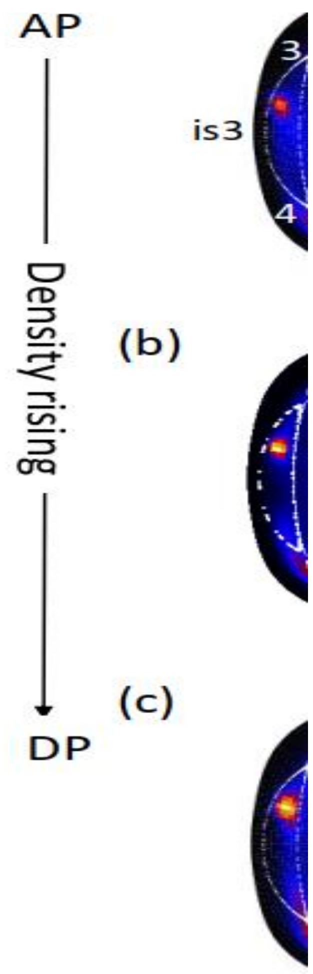

- Higher impurity radiation:
  - ✓ In IS3, in the upper partition

  → Corresponding to regions with upstream pol. **E**x**B** drift

Summary

- Plasma detachment induced by intrinsic carbon impurities have been routinely obtained in the ECR-heated plasma after boronization (OP1.2b) with standard magnetic configuration. It is characterized by a high radiation fraction (f_{rad}) with significantly reduced divertor heat load and particle flux.

- **In the detached plasma phase (f_{rad} =0.6-0.9),** the 2D radiation patterns obtained by Bolometer tomography has revealed multi-X-point radiation (XPR) structure in the triangular cross-section, which has an up/down symmetric magnetic topology. The **multi-XPR structures are with up/down asymmetry** and the brightest XPR appears near the upper X-point for the normal magnetic field direction. Reversing the B-field direction, the main (up/down) asymmetry turns its sign, implying that the drift effect plays a role.

- **In the deep DP phase (f_{rad} ~1),** the degree of **up/down asymmetry significantly reduces**, nearly all SOL power is homogenously dissipated via impurity radiation.

- Video cameras confirm the bolometer results and further show that the multi-XPR has a band structure around the X-lines and helically follows the field periods.

- A simplified model considering the influence of the poloidal **E×B** drift (V_d) on the impurity flow in the SOL shows that

- the poloidal drift potentially leads to an up/down asymmetry of impurity density in the SOL despite the symmetry magnetic topology:
  - ✓ **downstream drift toward the target or TSR (V_d <0) decreasing the impurity content,**
  - ✓ **upstream drift toward the LCFS (V_d >0) increasing the impurity content.**
- The dynamics of the up/down asymmetry in the multi-XPR structure is related to the magnitude V_d/D (normalized to the impurity diffusivity), with an additional effect owing to the radial inward shift of the emission zone.

Thanks for your attention!

Discussions: downstream CII emission profile

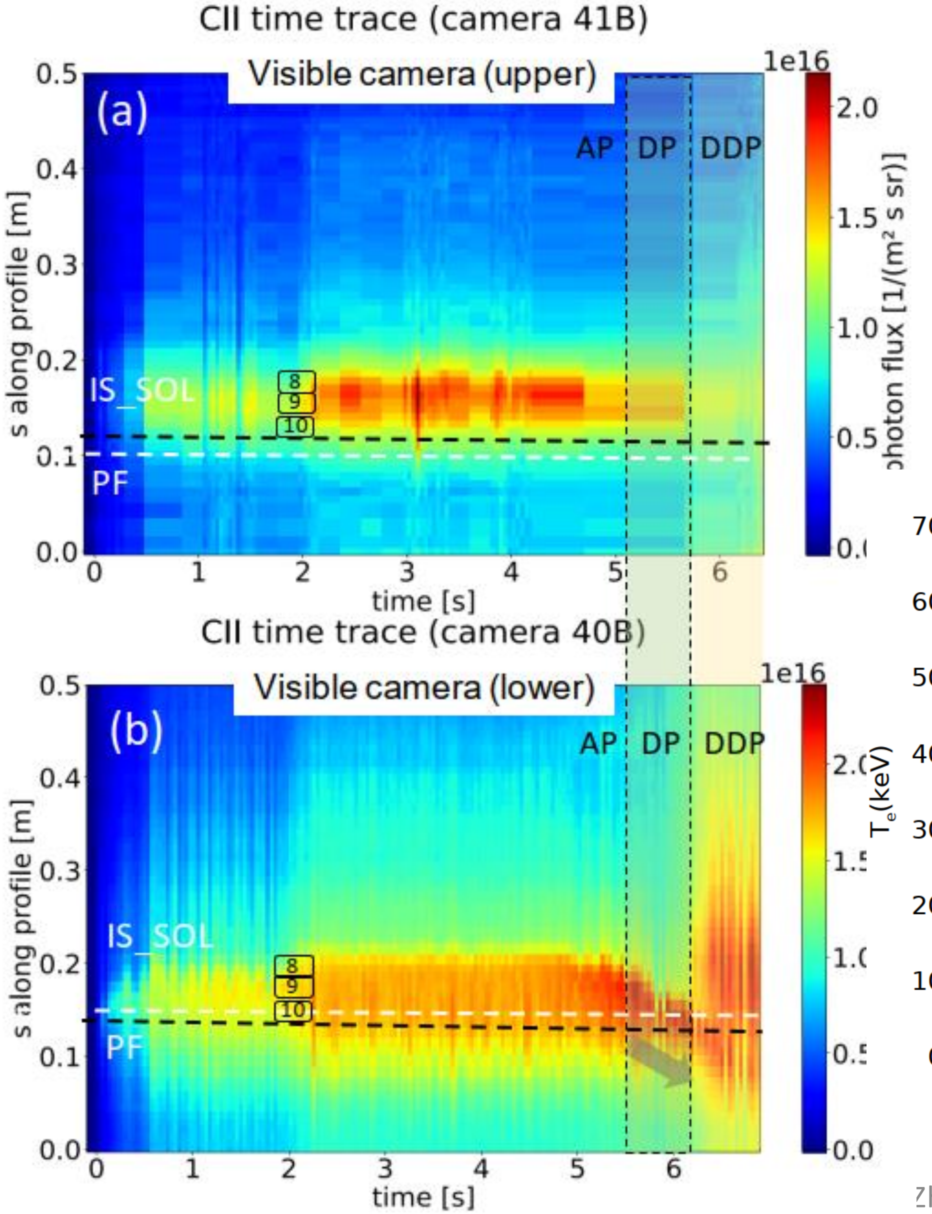

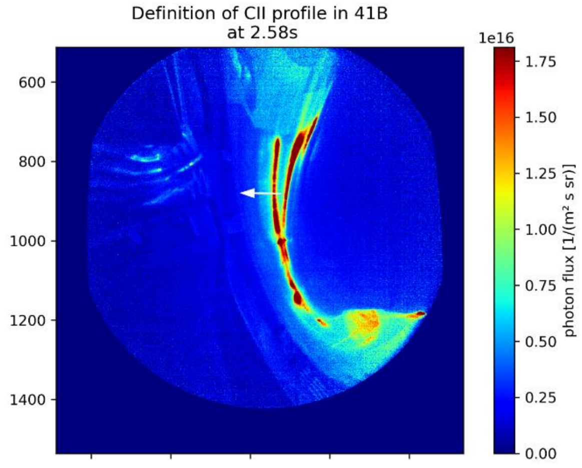

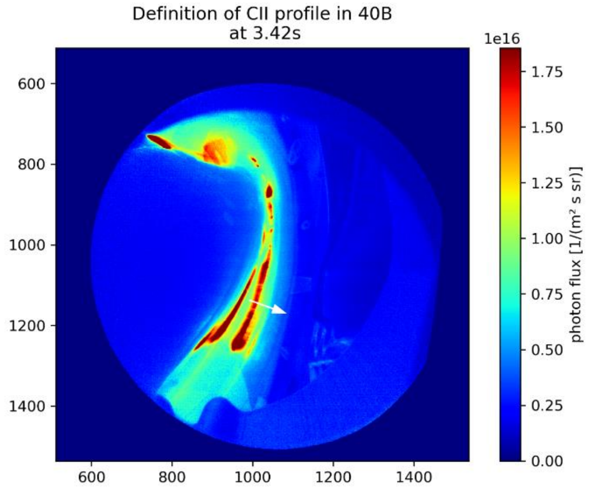

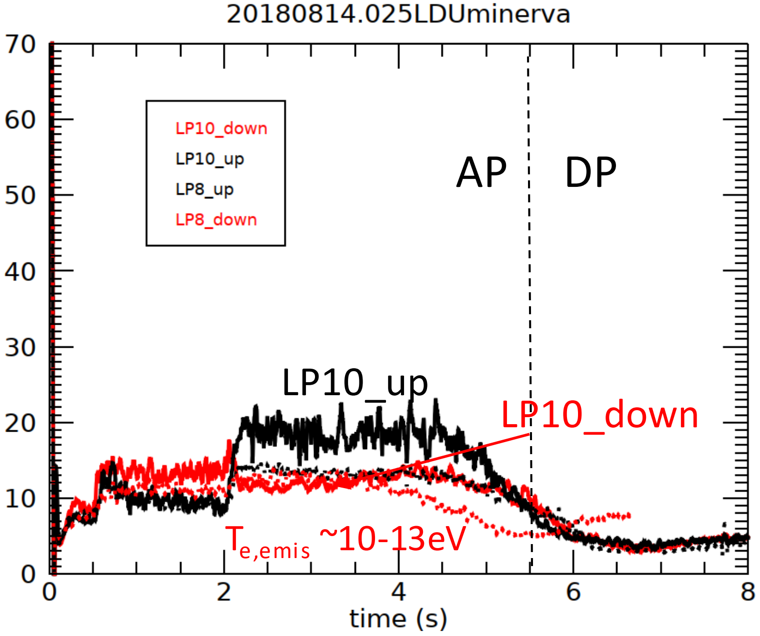

ε_{rad} (CII) $\propto n_z L_z$ (Te, z=1)

$\rightarrow Y\Gamma_i L_z$(Te, z=1)

Y: impurity yield due to physical and chemical sputtering

- ❑ **upper** profile **narrower**;
- ❑ lower SOL:

At DP phase, stronger CII emission

Discussions: Downstream CII emission profile vs. heat load profile

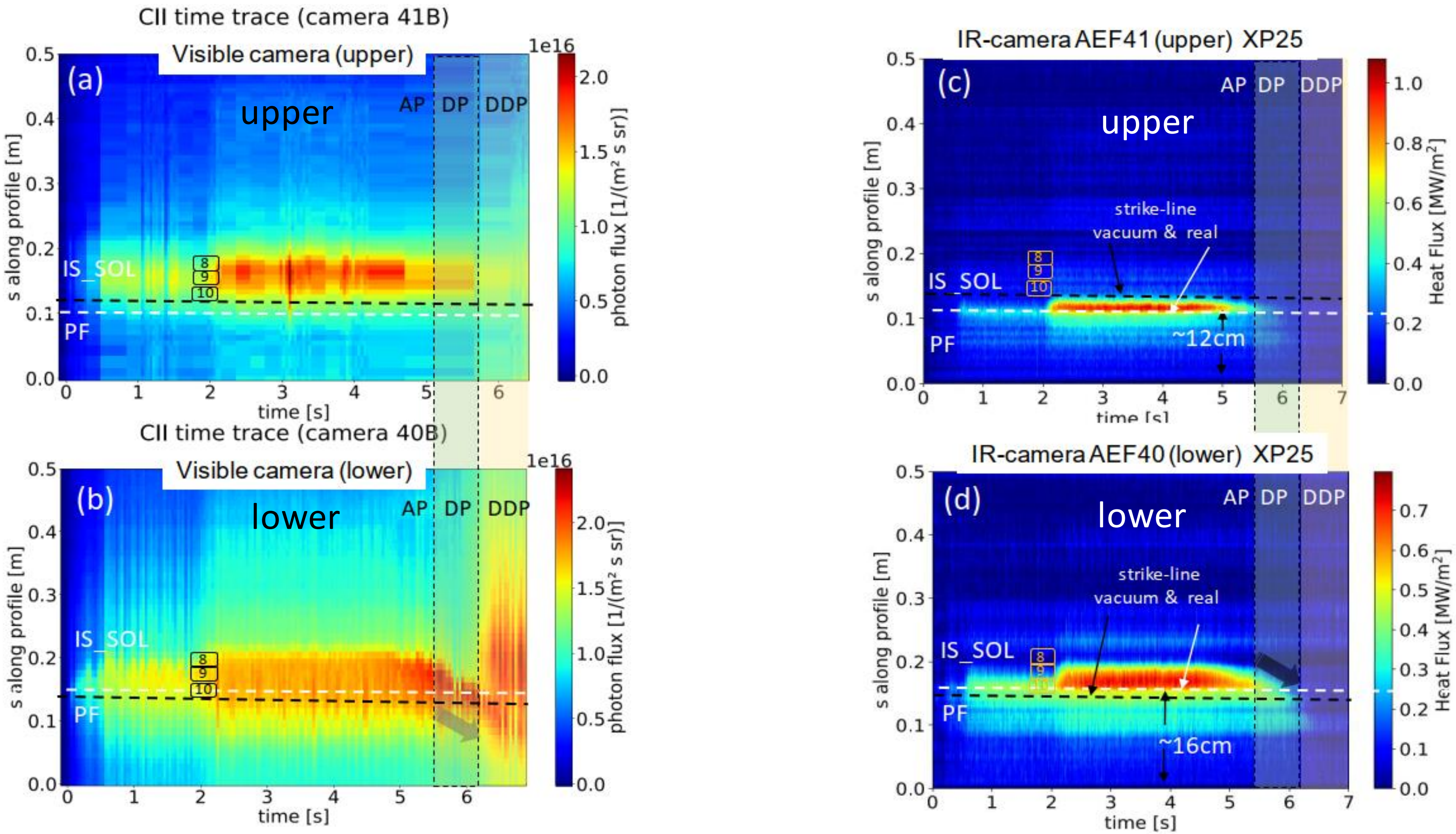

The up/down asymmetry

- both CII and heat flux profile near/on **the upper** targets are **narrower**

! error fields probably impact the strike line positions;

! Upper strike zone outside IS_SOL can not predicted by the simple model (slide 25).